Environmental Science and Pollution Research
https://doi.org/10.1007/s11356-025-36682-z

RESEARCH ARTICLE

Cost-effective biochar from spent coffee grounds as a sampling device of gaseous polycyclic aromatic hydrocarbons

Wittaya Tala[1,2] · **Suparin Chaiklangmuang**[3] · **Somporn Chantara**[1,2]

Received: 30 October 2023 / Accepted: 18 June 2025

Abstract

Biochar derived from spent coffee grounds was used for the first time as an adsorbent for monitoring and application in a sampling device of gaseous polycyclic aromatic hydrocarbons (PAHs), rather than for the removal of PAHs from the environment, as had been attempted in previous research. The device consists of three parts: an air filtration component, an air sampling component (glass tube filled with lab-made biochar), and a flow controller component. The findings demonstrated that the developed sampling device has a high potential for the collection of gaseous PAHs in ambient air, including naphthalene, acenaphthylene, acenaphthene, fluorene, phenanthrene, anthracene, fluoranthene, and pyrene, under conditions involving low air flow rates (≤ 4 L/min) and low temperatures (≤ 10 °C). Moreover, two connected glass sampling tubes packed with lab-made biochar performed better than a single tube and required less than three hours to prevent significant loss of gaseous PAHs. By using the spiking method on biochar prior to sampling, accuracy levels greater than 80% were achieved for all compounds. Additionally, the efficiency of the biochar was compared with that of a commercial adsorbent (XAD-2), and no significant differences were found. These results suggest that biochar has strong potential for practical applications in the sampling of gaseous PAHs. When comparing production costs, the average price of biochar produced from biomass was estimated to be around 0.18% of the cost of the commercial adsorbent (XAD-2) per sampling.

Keywords Air sampling · Biochar · Gas emission · Gaseous PAHs · Upper Southeast Asia · XAD-2

Introduction

Polycyclic aromatic hydrocarbons (PAHs) are a group of pollutants consisting of hydrocarbon compounds characterized by the presence of two or more fused aromatic rings. They are found in the atmosphere in both gaseous and particulate phases. PAHs with two to three rings are predominantly found in the gaseous phase, while those with five to seven rings are mainly present in the particulate phase. Four-ring PAHs, however, are distributed between both phases (Eiguren-Fernandez et al. 2007; Lu et al. 2008; Martins et al. 2013). In general, the health hazards associated with gaseous PAHs are lower than those posed by particulate PAHs. However, gaseous PAHs are more abundant in the environment (Romo et al. 2019). Acute exposure to these compounds can cause symptoms such as eye irritation, vomiting, diarrhea, confusion, skin irritation, and inflammation. Chronic health effects include eye cataracts, kidney and liver damage, respiratory issues, decreased immune function, lung dysfunction, and asthma-like symptoms (Abdel-Shafy and Mansour 2016). For example, naphthalene has been linked to headaches, cataracts, hemolysis, and renal damage (Nayak et al. 2019). It is also associated with dermatitis and cancer (Sukadi and Ilyas 2022). Additionally, Yang et al. (2019) reported that phenanthrene elevated CYP2B10 expression, leading to hepatotoxicity. Moreover, small-molecule PAHs have been found to suppress gap-junctional intercellular communication in cells more effectively than high-molecular-weight PAHs in living organisms (Romo et al.

Responsible Editor: Philippe Garrigues

✉ Wittaya Tala
witaya.tala@cmu.ac.th

[1] Environmental Science Research Center (ESRC), Faculty of Science, Chiang Mai University, Chiang Mai 50200, Thailand

[2] Environmental Chemistry Research Laboratory (ECRL), Department of Chemistry, Faculty of Science, Chiang Mai University, Chiang Mai 50200, Thailand

[3] Department of Industrial Chemistry, Faculty of Science, Chiang Mai University, Mai University, ChiangChiang Mai 50200, Thailand

Published online: 05 July 2025

2019; Wong et al. 2017). Under favorable conditions in the ambient air, these molecules can also transform into significantly more hazardous oxidized PAHs (Mueller et al. 2019; Ringuet et al. 2012). Drotikova et al. (2020) reported that the primary pathways for PAH degradation include direct photolysis and reactions with atmospheric oxidants—such as hydroxyl and nitrate radicals, ozone, and nitrogen dioxide—in the gas phase, as well as heterogeneous gas-particle interactions. Numerous studies have shown that oxidized PAHs are more harmful than their non-substituted counterparts, as they can cause DNA damage, mutations, and cancer (de Oliveira Galvão et al. 2018; Bandowe and Meusel 2017; Idowu et al. 2019).

The sampling of PAHs is typically conducted for both gaseous and particulate phases using a high-volume active air sampler that operates at a flow rate between 15 and 30 m^3/h (Kim Oanh et al.2000; Portet-Koltalo et al. 2007). In this method, the particulate phase is collected by trapping PAHs on a filter paper, while the gaseous phase is sampled by subsequently adsorbing PAHs onto materials such as polyurethane foam (PUF) (Bohlin et al. 2010; Meijer et al. 2008), Tenax TA (Sonnette et al. 2017; Wauters et al. 2008), or XAD resins (Kobayashi et al. 2010; Wei et al. 2007). However, several limitations are associated with this conventional approach, primarily due to reduced degrees of sampling efficiency. These issues result in blow-off (also called volatilization) and the effects of elevated temperatures, which can lead to significant losses of PAHs from the sampling media (Galarneau and Bidleman 2006), as well as in incidences of oxidation by atmospheric gases (Chu et al. 2010).

Over the past decade, various alternative sampling methods have been developed and employed for monitoring gaseous PAHs in ambient air. Among these, passive sampling methods have been advanced with wider applications for our proposed objective (Bartkow et al. 2005; Choi et al. 2009; Namieśnik et al. 2005). Compared to high-volume active air sampling, passive sampling offers several advantages: it is cost-effective, compact, simply constructed, and easy to operate and transport and does not require electricity. However, this technique also has certain limitations. It typically requires extended sampling durations, while the collected analytes are susceptible to photodegradation and oxidation by atmospheric oxidants.

To improve sampling efficiency, some researchers have introduced an alternative method for collecting gaseous PAHs using low-flow active sampling (1–3 m^3/h) through various sorption media such as polydimethylsiloxane (PDMS) foam/PDMS particles/Tenax TA (Wauters et al. 2008), PDMS/Tenax TA (Lazarov et al. 2013), and water + surfactant (Portet-Koltalo et al. 2007). This approach has demonstrated greater sampling efficiency by minimizing the loss of volatile compounds and significantly reducing the risk of contamination. However, monitoring gaseous PAH compounds in the ambient air using this method requires large quantities of commercial sorbent media, resulting in high operating costs and other recurring expenses, which make it unsuitable for widespread applications in many developing countries. As a result, the development of cost-effective alternative sampling materials and methods is considered both necessary and urgent.

Biochar (BC) is recognized as a low-cost adsorbent produced from a variety of abundant carbon-rich biomass forms of waste, such as agricultural and forest residue, as well as from animal residue. It is generated through a thermochemical process in the absence of oxygen at relatively low temperatures (≤ 700 C) (Lehmann and Joseph 2009). Recently, BC has attracted considerable attention due to its beneficial properties, which include a large specific surface area, highly porous structure, enriched surface functional groups, and a diverse mineral composition (Cao et al. 2017; Han et al. 2017). As a result, it has been effectively utilized in a range of environmental, agricultural, and horticultural applications (Dumroese et al. 2011).

To our knowledge, only a small number of studies have reported the use of biochar (BC) as an adsorbent with good adsorption capacity for polycyclic aromatic hydrocarbons (PAHs) in soil and aqueous media (Lamichhane et al. 2016; Zand 2017), while none have specifically investigated its application for gaseous PAH sampling. This research, therefore, aimed to develop a highly efficient sampling device for gaseous PAHs using BC derived from spent coffee grounds as a low-cost adsorbent. One of the main challenges in gaseous PAH sampling is the loss of analytes at various stages, particularly during sampling. Accurate quantification requires low-volume active air sampling, with performance highly dependent on the sorbent material used. In this study, BC was selected as the sorbent for gaseous PAH collection, and a dedicated method was developed to optimize its sampling efficiency. The device was subsequently validated under real field conditions to address the challenges posed by complex sampling matrices during a smoke haze period.

Materials and methods

Chemicals and standards

A 2000 µg/mL PAH standard (99% purity in dichloromethane) was employed in this research study. It contained the following components: naphthalene (NAP), acenaphthylene (ACY), acenaphthene (ACE), fluorene (FLU), phenanthrene (PHE), anthracene (ANT), fluoranthene (FLA), pyrene (PYR), benzo[a]anthracene (BaA), chrysene (CHR), benzo[b]fluoranthene (BbF), benzo[k]fluoranthene (BkF), benzo[a]pyrene (BaP), dibenz[a,h]anthracene (DbA), indeno

[1,2,3-cd]pyrene (IND), and benzo[g,h,i]perylene (BPER). This standard was supplied by Restek Corporation (Bellefonte, PA, USA). Additionally, a 2000 µg/mL deuterated internal standard acenaphthene-d_{10} (ACE-d_{10}) (99% purity in dichloromethane) was obtained from Supelco (Mainz, Germany). Both standards were diluted to prepare stock solutions at concentrations of 20 µg/mL for the reference standard and 50 µg/mL for the internal standard using a hexane (Hex):dichloromethane (DCM) (1:1, *v/v*) mixture. All organic solvents used in this research project were of high-performance liquid chromatography (HPLC) grade (99.9% purity) and were obtained from RCI Labscan (Bangkok, Thailand). The solvents were stored in amber bottles at − 20 °C to prevent photodegradation of PAHs.

Experimental apparatus and procedure

BC was produced from spent coffee grounds (SCGs) in a fixed bed reactor. In each of our trials, 60 g of dried SCGs was used for each experiment (Supplementary Fig. A.1). Nitrogen gas was introduced into the reactor at a heating rate of 50 °C/min for 30 min to ensure complete removal of oxygen (O_2) from the system. Pyrolysis was then conducted at target temperatures of 300 °C and 500 °C, while a consistent heating rate of 10 °C/min was applied. Each temperature was held for 1 h before the system was allowed to cool to room temperature. The resulting biochar were designated as BC300 and BC500, which corresponded to the SCGs pyrolyzed at 300 °C and 500 °C, respectively.

Physicochemical characterization

Sample preparation

Since physicochemical characterization requires clean, pure, and dry samples, the specimens, referred to as samples in the context of physicochemical characterization, were placed in an oven at 60 °C for 24 h to minimize residual moisture. They were then stored in a desiccator for at least 24 h before being used.

Characterization method

The physicochemical properties of SCGs and BC were examined using the following methods:

(i) *Thermal decomposition behavior* was analyzed to measure the quantity and rate of mass change due to breakdown, oxidation, or dehydration as a function of temperature or time. This was performed using thermogravimetric analysis (TGA) and the first derivative of the TGA curve. Accordingly, the rate of mass loss as a function of temperature or time was examined using derivative thermogravimetry (DTG). Both analyses were conducted simultaneously with a PerkinElmer TGA7 (USA). To prepare samples at temperatures ranging from 50 to 1300 C, a platinum (Pt) macro pan with a maximum temperature tolerance of about 1500 C was used. Two pans were employed: one for reference and one for the sample. After balancing the instrument between the reference and sample pans to account for the weight of the reference pan, only the sample pan was removed, filled with a specimen weighing less than 20 mg, and placed in the designated sample site within the instrument. The temperature was set between 50 and 1300 C with a heating rate of 10 C per minute in a nitrogen atmosphere prior to analysis.

(ii) *Specific surface area* was determined by nitrogen (N_2) adsorption and calculated using the Brunauer–Emmett–Teller (BET) method with a Quantachrome Autosorb-1 analyzer (USA). An important step in the process involved carefully recording the mass of each specimen by subtracting the mass of an empty gas rod from that of the gas rod filled with the specimen. This was done in order to determine the sample weight before degassing. Each specimen was then degassed in the BET analysis instrument overnight prior to beginning the analysis. After degassing, the specimens were immersed in a liquid nitrogen bath while the instrument conducted the nitrogen adsorption tests. During the test, known quantities of ultra-pure nitrogen gas were introduced into the tube, while the relative pressure (P/P_0) was recorded. This measurement was limited to a specific region of the adsorption isotherm, typically within a P/P_o range of 0.05 to 0.35. The collected data were then used to calculate the mass-specific surface area of the material, with automated calculations performed by the software based on a linear plot of $1/[(P_0/P) - 1]$ vs. P/P_0, as has been presented in Eqs. (1) and (2).

$$\frac{1}{\upsilon\left[\left(\frac{p}{p_0}\right) - 1\right]} = \frac{c - 1}{\upsilon_m c}\left[\frac{p}{p_0}\right] + \frac{1}{\upsilon_m c} \tag{1}$$

where υ is the adsorbed volume of gas, υ_m is the adsorbed monolayer volume, p is the equilibrium gas pressure, p_0 is the saturation pressure, and ccc is the BET constant. The *Y*-intercept and slope of this function can then be used to solve for the constants c (= slope/intercept + 1) and υ_m (1/(slope + intercept). The specific surface area (*S*, surface area per unit mass) can then be calculated using the following equation:

$$S = \frac{\upsilon_m NA}{22{,}400xm} \quad (2)$$

where N is Avogadro's number (molecules per mole), A is the cross-sectional surface area of a single adsorbed gas molecule, mmm is the mass of the nanomaterials used in the measurement, and 22,400 is the Standard Temperature and Pressure (STP) volume of one mole of gas. The surface area is expressed in units of area per mass (e.g., m^2/g), which can be converted to a volume-specific surface area through multiplication of the material's density.

(iii) *Surface functional groups* were identified using Fourier-transform infrared spectroscopy (FT-IR) with a BRUKER Tensor 27 instrument (Germany). The process involved the following steps: Prior to processing, each piece of equipment was cleaned with absolute ethanol. A sample of 1.0–2.0 g was gently ground with 200 mg of solid KBr using an agate mortar and pestle to form a fine powder. This mixture was then pressed into a pellet under a vacuum and at a pressure of about 75 kN/cm^2 for 2–3 min to produce a clear and transparent pellet. These pellets were placed in the sample holder of the FTIR instrument for spectral analysis of the functional groups. The spectral resolution was 4 cm^{-1} with a scanning range of 400–4000 cm^{-1}.

(iv) *Surface morphology* was observed using scanning electron microscopy (SEM) with a JEOL JSM-5910LV (USA). Specimen current is a key characteristic of electron-sample interaction, as changes in specimen current can significantly influence imaging quality. To regulate and enhance imaging, electro-conductive tape should be used, and the samples should be coated with conductive material. Specimens were mounted on the surface of the stub using double-sided carbon adhesive tabs (tape). Compressed air was used to remove any excess material to prevent contamination of the SEM instrument and maintain vacuum integrity. The specimens were then coated with gold using a gold sputtering system. After sputtering, the stub was removed from the system before inserting the sample into the SEM instrument. Next, the pumps were activated, allowing the system to reach the required vacuum conditions. The SEM software was then launched, and a focused image of each sample was acquired at magnifications of 250x, 1000x, and 2500 × to compare the morphology of each compound.

Field validation of a developed gaseous PAH sampling device

Design of gaseous PAH sampling device

The low-volume active air sampling device was designed to collect gaseous PAHs in ambient air and consisted of three main components: Part I (Air introduction component), Part II (PAHs sampler), and Part III (Flow controller) as shown in Fig. 1. These components are connected via a nylon tube, which was chosen for its elasticity and capacity to handle oil and chemicals, as well as its durability and ability to maintain a constant flow. In the operation, air samples were continuously drawn through a sheet of cellulose acetate paper (0.8-μm pore size) in Part I. In Part II, the gaseous PAH compounds were adsorbed by selected adsorbents such as XAD-2 or BC. This part was developed to minimize the loss of gaseous PAH compounds by operating at low temperatures. To maintain a stable temperature during sampling, a gas sampling tube, filled with adsorbents, was placed inside a polyvinyl chloride (PVC) pipe, which was then packed inside a foam box. Ice packs were used to regulate the temperature of the sampling tubes, as they are relatively inexpensive, easy to acquire, and reusable. The temperatures within the sampling unit were kept constant at around 8–10 °C and were controlled as necessary.

The flow controller (Part III) consisted of a flow meter and a vacuum pump. The gaseous PAH compounds were adsorbed onto the glass surface, which resulted in a loss of analytes. To prevent this, the sampling tubes were soaked in isopropanol to coat the glass surface. Afterward, the tubes were dried, and the adsorbent was packed.

Sampling tubes and adsorbents

Two types of adsorbents (XAD-2 and BC) were selected to compare the collection of gaseous PAHs obtained from ambient air. The commercial XAD-2, with a specific surface area of 346.6 m^2/g, was bought from Sigma-Aldrich-Supelco Chemical Co., Ltd. (USA), while BC was produced by slow pyrolysis of SCGs. A glass pasteur pipette (150-mm length × 0.9-mm i.d. × 2-mL volume; Paul Marienfeld GmbH & Co. KG, Germany) was used as an adsorbent package, as shown in Fig. 1. The results obtained from a sample tube containing 250 mg of BC, which was the largest amount used for the gaseous extraction of PAHs by ultrasonic extraction, showed no significant difference (Tala and Chantara 2019b) when compared with the results of a sample tube containing 150 mg of XAD-2 as a standard adsorbent (NIOSH method 5515) (NIOSH 1994). The tubes were then set up in the

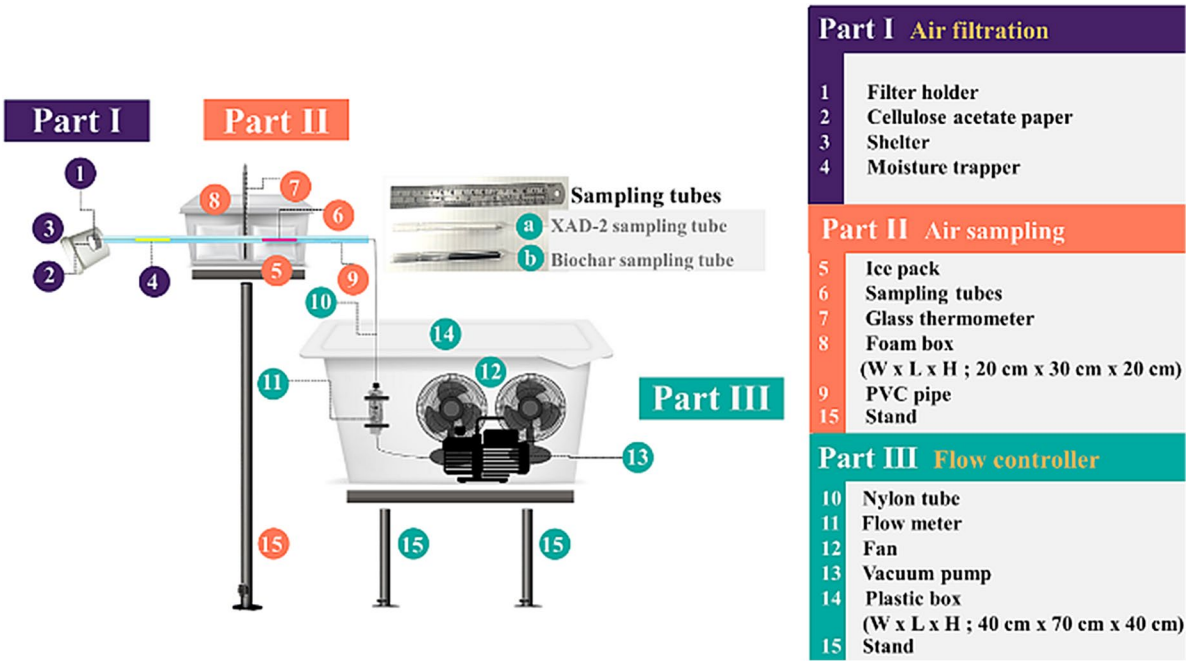

Fig. 1 Schematic diagram of low-volume active air sampling for gaseous PAHs. Part I: air filtration, Part II: air sampling, and Part III: flow controller

complete sampling device to collect gaseous PAHs from the ambient air on the rooftop of a 9-storey building (ScB1), Faculty of Science, Chiang Mai University (CMU), Thailand, during a smoke-haze period in northern Thailand.

Sample treatment and analysis

Sample treatment of PAHs was developed for both extraction and sample clean-up to facilitate the study of trace compounds in a wide range of sample matrices adsorbed onto both adsorbents prior to GC–MS analysis (Tala and Chantara 2019a). Eight PAHs (2- to 4-ring compounds) were selected, including NAP, ACY, ACE, FLU, PHE, ANT, FLA, and PYR because they vaporize rapidly at ambient temperatures (30–45 °C) and within a short sampling period. All resulting factors and outcomes were aligned with this study's objectives. In brief, the eight PAHs adsorbed onto the adsorbents (i.e., BC and XAD-2) were extracted using ultrasonic extraction. During the process, each sampling adsorbent was soaked in 25 mL of a mixture of dichloromethane (DCM):2-propanol (2-pro) (4:1) for about 5 min and ultrasonicated for 30 min at a low temperature (≤ 10 °C). The extract solution was then filtered through a 0.45-µm nylon syringe filter (Agela, USA) before being reduced to approximately 0.80–1.0 µL using a rotary evaporator. The solution was adjusted to 2.0 mL with a mixture of 2-pro: water (1:1) to protect the analytes from volatility and adsorption on a glass container before it was stored in a refrigerator until analysis. Prior to GC–MS analysis, co-extracted compounds and any remaining water in the extract solution were removed. The solution was diluted with 4.0 mL of water to obtain 20% 2-pro in water, which helped maintain activation of the octadecyl chains on the sorbent bed for solid-phase extraction (SPE) during the clean-up process. The solution was then cleaned up using a silica-based SPE cartridge, and 3.0 mL of a DCM: Hex:2-pro (1:1:0.1) mixture was used as the eluent. An excess of anhydrous Na_2SO_4 (about 250 mg), which was sufficient to remove the water bubble from the solution, was added to completely remove the water before filtration through a 0.45-µm nylon syringe filter. The syringe filter was then rinsed with 5–10 mL of the eluent to reduce analyte sorption. The solution was subsequently concentrated again using a rotary evaporator.

Finally, 200 µL of 0.020 µg/mL of ACE-10 (internal standard) was added to achieve a final concentration of 0.020 µg/mL in a 2-mL volumetric flask prior to GC–MS analysis. The efficiency of the sample treatment was then evaluated by recovery values of the 8 PAHs using a spiking method and SRM 1649b. The spiking method recovery values ranged from 81% (NAP) to 96% (ANT), while SRM 1649b recovery values ranged from 64% (NAP) to 98% (ACY and FLU) (Tala and Chantara 2019a).

Quality assurance/quality control for analysis of gaseous PAHs by GC/MS

To verify the capability of the sampling device for gaseous PAHs, key analytical parameters of GC–MS, including a calibration graph, limit of detection (LOD), limit of quantification (LOQ), linearity, and precision, were investigated. Calibration graphs were constructed for each PAH, covering both low concentrations (0–20 ng/mL) and high concentrations (10–100 ng/mL). LOD and LOQ were determined by an injection of 10 times the lowest concentration (1 ng/mL) of the mixed standard into GC–MS under optimum conditions. The values for LOD and LOQ were then calculated from both 3- and 10-times standard deviations for LOD and LOQ, respectively. The degree of precision, in terms of repeatability and reproducibility, was evaluated by performing 10 injections of the same standard on the same day and after 10 days, respectively. The results were presented in terms of % RSD (relative standard deviation). All data have been presented, and an evaluation of the sampling device for the gaseous PAHs was also obtained (Tala and Chantara 2019b).

Results and discussion

Physicochemical characterization of BC

Thermogravimetric analysis (TGA)

An earlier study (Kreatananchai et al. (2015) attempted to increase the value of SCGs as a feedstock for BC production to promote fuel generation. To determine the optimal pyrolysis temperature, thermogravimetric analysis (TGA) was employed to investigate the mass loss of SCGs as a function of temperature. Cellulose, hemicellulose, and lignin are the primary components of natural lignocellulosic materials. Accordingly, the composition of SCG was reported to consist of cellulose (8.6–47.3%), hemicellulose (32.0–43.0%), and lignin (23.9–33.6%) (Lee et al. 2023). These compounds degraded at different temperatures: hemicellulose between 220 and 300 °C, cellulose between 300 and 340 °C, and lignin above 340 °C (El-Sayed and Mostafa 2020). Based on the decomposition profiles and weight loss trends established from TGA, pyrolysis temperatures of 300 °C and 500 °C were selected for BC production. The resulting BC yields were 73.00% and 34.67% for BC300 and BC500, respectively, indicating a two-fold reduction in yield at the higher temperature. However, at 500 °C, the remaining BC was primarily composed of lignin, which possessed aromatic rings with hydrophobic properties. This enhanced its potential to adsorb PAHs via π-π electron-donor–acceptor interactions, while also contributing to a lower degree of water adsorption (Crocker 2010; Liu et al. 2010a). At this temperature, polar active sites originating from cellulose and hemicellulose were largely degraded, further promoting hydrophobic adsorption. Notably, higher pyrolysis temperatures resulted in BC that is more thermally stable and hydrophobic (Wan Ab Karim Ghani et al. 2013). However, the trade-off is a reduced yield that must be considered for commercial-scale applications due to ever-increasing production costs. In addition, the derivative thermogravimetric (DTG) plot showed that thermal degradation of SCGs occurred primarily between 200 and 600 °C, with more than 95% devolatilization achieved at 500 °C. Therefore, slow pyrolysis at this temperature was selected to maximize the effectiveness of BC for gaseous PAH adsorption following fuel production. This pyrolysis temperature is also in agreement with those recommended for BC in environmental applications (Song and Guo 2012).

SEM analysis

The slow pyrolysis process of BC employed 125–355 µm dried SCGs as feedstock, which were then pyrolyzed at temperatures of 300 °C and 500 °C. After pyrolysis, the resulting BCs were found to have smaller particle sizes than the original SCGs due to the thermal degradation of organic components. The particle sizes were approximately 180 µm for BC300 and 125 µm for BC500. According to Tala and Chantara (2019b), the surface morphology of raw SCGs exhibited smooth and thick plate-like structures, indicating a lack of porous structure and low specific surface area. This was likely because the active sites and pores were covered by volatile organic compounds (Pignatello et al. 2006). In contrast, the SCGs pyrolyzed at 300 °C (BC300) and 500 °C (BC500) displayed surfaces with various pore structures. This could have been attributed to the release of volatile compounds during pyrolysis, which generated new pores, thereby increasing the surface area and pore volume and enhancing physical adsorption (Lin et al. 2014; Omidi et al. 2019; Wang et al. 2015). Notably, BC500 exhibited more extensive pore formation than BC300 due to the higher degree of volatile compound removal that occurred at the elevated temperature. This would also suggest that the pyrolysis temperature significantly influenced the pore structure, affecting not only the number of pores, but also wall thickness and pore diameter size (Fu et al. 2011; Liu et al. 2010b). Therefore, the morphology of BC500 differed markedly from that of BC300. However, nitrogen adsorption analysis revealed that both B300 and B500 had relatively low specific surface areas. This could have been due to the residual bio-oil present on the surfaces of the BCs, which may have interfered with the adsorption and desorption processes. Therefore, BC derived from SCGs should always be cleaned prior to use as an adsorbent in monitoring applications.

Specific surface area

The Brunauer–Emmett–Teller (BET) method was used to determine the specific surface area of both BC and SCGs. According to Tala and Chantara (2019b) the specific surface areas of BC300 and BC500 were found to be 4.58 m^2/g and 8.42 m^2/g, respectively. These values are consistent with those reported in previous studies for other biomass sources, such as buckwheat husk (10.7 m^2/g) (Zama et al. 2017), corn stover (3.1 m^2/g) (Mullen et al. 2010), and fescue straw (1.8 m^2/g) (Keiluweit et al. 2010). Several factors contributed to the relatively low specific surface area observed in this study: (i) the presence of inorganic materials that partially filled or blocked the residual pores, (ii) limited N_2 accessibility into the micropores of BC, (iii) bottleneck-shaped pores and a low abundance of slit shape, (iv) nonlinear behavior in the low to mid-pressure range of the BET isotherm, and (v) a non-equilibrium state in the N_2 adsorption–desorption process, potentially caused by surface-bound bio-oil. The bio-oil, a sticky residue presents in both BC300 and BC500, likely served as a barrier to nitrogen molecules during BET measurement, which also contributed to the non-equilibrium adsorption–desorption behavior. Although these BET values are useful for comparing BC produced under similar conditions, the BC produced in this study was intended for use as an adsorbent for gaseous PAHs. Therefore, it was necessary to clean the BC in order to remove residual PAHs and any other contaminants. According to Spicer et al. (1990), the acceptable level of PAHs in adsorbents should be below5 µg/g. In this study, the residual PAHs in the cleaned BC ranged from 0.064 to 0.070 µg/g. Following the cleaning process, the specific surface areas increased significantly from 4.58 to 37.15 m^2/g for BC300, and 8.42 to 98.32 m^2/g for BC500. These results indicate that without the cleaning step, bio-oil residues would have continued to inhibit nitrogen adsorption–desorption, leading to underestimated BET surface area values.

Fourier-transform infrared (FTIR)

Fourier-transform infrared spectroscopy (FTIR) analysis revealed that the functional groups present in BC were predominantly linked to oxygenated hydrocarbons, which originated from the structure components of cellulose and hemicellulose (Wan Ab Karim Ghani et al. 2013). According to Tala and Chantara (2019b), the FTIR spectra showed evidence of aliphatic compound degradation, as indicated by the disappearance of aliphatic C-H stretching in 2950–2850 cm^{-1} and C-O stretching in 1135–952 cm^{-1} ranges in both pyrolyzed BC300 and BC500. In addition, prominent bands corresponding to aromatic carbon structures were observed. These included C-H stretching within a range of 860–680 cm^{-1}, C = C bending within a range of 1700–1500 cm^{-1}, and C = O stretching within a range of 1750–1680 cm^{-1}, which were especially evident in both BC300 and BC500. The increased presence of aromatic C groups in the IR spectra suggests enhanced aromaticity, which has been linked to improved PAH adsorption capacity (Lee et al. 2010). Accordingly, these alterations may have led to higher levels of PAH adsorption on the adsorbent (Lee et al. 2010) and greater resistance to oxidation and degradation (Spokas et al. 2009), as has been reported by Keiluweit et al. 2010. Moreover, characteristic bands of silicon dioxide (SiO_2) were observed at 460, 800, or 1040–1100 cm^{-1} in both SCGs and BC, indicating the presence of phytoliths–silica-based structures that naturally occur in plants tissues (Parr 2006). Silicon (Si), the second most common element in the Earth's crust, is typically found in high amounts in soil samples (> 50% SiO_2). It plays an essential role in plant physiology by mitigating environmental stresses through its function as a bio-silicon within the soil–plant system. It is primarily adsorbed by the roots of plants (Matichenkov and Bocharnikova 2004: Mitani et al. 2005). Si accumulates in epidermal tissue and forms a cellulose membrane-Si layer when calcium and pectin ions are present (Waterken et al. 1981). Therefore, it is not surprising that Si was detected in the resulting BC produced from plant-based feedstock. BC enriched with silicon, often referred to as "Sichar," has shown promise in soil improvement and environmental remediation applications, such as by alleviating aluminum (Al) toxicity in plants and immobilizing contaminants like arsenic (As), cadmium (Cd), and hexavalent chromium [Cr (VI)] (Wang and Wang 2019).

Optimization of sampling conditions affecting collection efficiency

Sampling flow rate

Flow rate is a key parameter that affects the efficiency of the sampling process, as it influences the resident time of the gaseous PAHs adsorbed on the adsorbents (Jin et al. 2014; Temime-Roussel et al. 2004). To obtain sufficient quantities of PAHs, high-volume active air samplers are typically employed to simultaneously collect gaseous and particulate PAHs at specific high flow rates (1–−30 m^3/h) (Kim Oanh et al.2000; Portet-Koltalo et al. 2007); however, there are a number of limitations that can be associated with high losses of compounds. In this research study, the sampling process was significantly improved by implementing a low-flow-rate system for gaseous PAH sampling. Consequently, the optimal low flow rate for the developed gaseous PAH sampling device was firstly investigated. The commercial adsorbent (XAD-2), used as a reference according to the NIOSH Method 5515 (NIOSH 1994), was tested at a flow rate of 2 L/min, while BC500 was evaluated at flow rates

of 2, 3, and 4 L/min. Given the likely lower adsorption potential of BC500 when compared with XAD-2, this study aimed to enhance the performance of BC500 for gaseous PAH adsorption, wherein we strived to achieve a degree of efficiency comparable to that of XAD-2. This challenge was addressed by incorporating a moisture trap tube installed before the BC500 sampling tube to remove moisture and polar compounds, as well as by employing a low-temperature system to reduce evaporation rates while ensuring effective adsorption of gaseous PAHs on both adsorbents. Following Chuang et al. (1987), lower temperatures were found to yield higher recovery values of volatile PAHs during sampling. The estimated degrees of efficiency of BC500 and XAD-2 at different flow rates were compared using the ratios of BC500 to XAD-2 (B/X) for individual rings of PAHs. All ratio values were close to 1, indicating that the efficiencies of both adsorbents were nearly identical. As is shown in Table 1, the ratios of gaseous PAHs obtained from BC500 and XAD-2 sampling tubes varied as follows: 0.67–0.86 for 8-PAHs, 0.64–0.94 for 2-ring PAHs, 0.69–0.86 for 3-ring PAHs, and 0.78–1.14 for 4-ring PAHs. These variations may be attributed to differences in the physical properties of each adsorbent, such as surface area and surface functional groups, which could then affect sampling efficiency. Another important factor to consider is potential interference within the air sample, including moisture and polar compounds. These interfering substances may compete for adsorption sites on the heterogeneous surfaces of the adsorbents, leading to variations in the adsorption rates of gaseous PAHs, especially for biochar. However, this developed sampling method indicated that PAHs could be highly adsorbed on both kinds of adsorbents. Moreover, gaseous PAH concentrations obtained from various flow rates were not found to be significantly different. The adsorption that occurred on the glass surface of the sampling tube during the course of this research study should also be considered. This process is influenced by the retardation factor (R_f), defined as

$$R_f = \frac{(t - t\prime)}{(t_0 - t\prime)} \tag{3}$$

where t_0 is the dead time of the system, t is the measured retention time, and t' is the adjusted time. This equation indicates that the retardation factor depends on the travel time of a compound within the studied column, as well as on the sorption coefficient (K_d), which is defined as

$$K_d = \frac{C_s}{C_w} \tag{4}$$

where C_s is the equilibrium concentration of the compound on the glass surface and C_w is the equilibrium concentration of the compound in the media. According to Qian et al. (2011), flow rate should be selected with the goal of performing the experiment as quickly as possible. This is because a lower flow rate can increase the retardation factor (R_f) of the compound in any glass column. That, in turn, results in a higher sorption coefficient (K_d), where the adsorption of PAHs approaches equilibrium and a higher degree of adsorption on the glass surface can be observed. Therefore, both the length of the sampling tube and the sampling flow rate are important considerations. Moreover, according to Zheng et al. (2024), who studied the mass transfer kinetics of compound desorption from an adsorbent, penetration curves were plotted as $C_{ou}t/C_o$, where C_{out} is the concentration at the outlet of the fixed bed during the adsorption–desorption process (in mg/Nm^3) and C_o is the concentration of the compound at the inlet (also in mg/Nm^3) measured against time (seconds). The overall mass transfer coefficients determined under experimental conditions followed similar trends: when a high flow rate of gas passed through the packed bed of the adsorbent, the ratio of C_{out}/C_o was lowest, indicating that the adsorbate was more effectively adsorbed onto the adsorbent within the packed bed reactor. The results of mass transfer resistance, as studied by Ouchi et al. (2019), also indicated that overall mass transfer resistance decreased rapidly with an increase in air velocity, particularly during the adsorption process. This suggests that a greater amount of adsorbate was adsorbed onto the adsorbent and that the effective diffusivity was highest at high velocity. As has been previously established, a shorter sampling tube and a higher sampling flow rate are preferred to minimize losing effects. However, since only one size of glass tube was selected, flow rate was only one factor used in the estimation process. Therefore, a flow rate of 4 L/min was chosen as the optimal sampling flow rate for developing an effective sampling device for gaseous PAHs in ambient air. Importantly, based on previously published data, gaseous PAHs have not yet been investigated in Northern Thailand. Therefore, in this study, the sampling volume was carefully selected to ensure the successful detection of all eight target gaseous PAHs throughout the experiment. This decision was guided by the sampling flow rate, a critical parameter for field validation of gaseous PAH sampling. To further enhance accuracy and minimize matrix effects—factors that can compromise analytical reliability—as well as to reduce the potential loss of gaseous PAHs during collection, a short sampling duration with an optimized flow rate was employed. This strategy enabled the effective detection of very low concentrations of all eight gaseous PAHs present in the ambient air.

When compared with other studies on the development of gaseous PAH determination (low-volume active air sampling) and generally high-volume active air sampling (as is shown in Table 2), our selected flow rate aligns with the values reported in various other studies that aimed to develop active sampling methods for gaseous PAHs using low flow

Table 1 Effect of sampling flow rate and sampling time on adsorbent efficiency for gaseous PAHs device in the ambient air

		Detected gaseous PAHs (ng/m^3)								
		Mean ± SD (n = 3)								
Parameter	Sampling flow rate	**PAHs**	**Flow rate (2:2)**		***Ratio (B/X)***	**Flow rate (3:2)**		***Ratio (B/X)***	**Flow rate (4:2)**		***Ratio (B/X)***
			BC	**XAD-2**		**BC**	**XAD-2**		**BC**	**XAD-2**	
			2 L/min	**2 L/min**		**3 L/min**	**2 L/min**		**4 L/min**	**2 L/min**	
		2-ring PAHs	136 ± 18^a	156 ± 25^a	***0.87***	159 ± 16^a	220 ± 38^a	***0.74***	71 ± 42^a	102 ± 62^a	***0.71***
		3-ring PAHs	86 ± 10^a	117 ± 22^a	***0.74***	71 ± 5^a	90 ± 2^b	***0.79***	63 ± 6^a	76 ± 9^b	***0.83***
		4-ring PAHs	11 ± 4^a	12 ± 3^a	***0.86***	10 ± 2^a	13 ± 3^a	***0.84***	13 ± 3^a	14 ± 3^a	***0.98***
		8 PAHs	233 ± 23^a	286 ± 46^a	***0.82***	241 ± 15^a	322 ± 39^a	***0.75***	147 ± 39^a	192 ± 59^a	***0.78***
	Sampling time	**PAHs**	**Flow rate 4 L/min**		***Ratio (1 h/2 h)***	**Flow rate 4 L/min**		***Ratio (2 h/3 h)***	**Flow rate 4 L/min**		***Ratio (3 h/4 h)***
			BC			**BC**			**BC**		
			1 h	**2 h**		**2 h**	**3 h**		**3 h**	**4 h**	
		2-ring PAHs	*24 ± 2^a*	*33 ± 3^b*	***0.74***	*10 ± 1^a*	*15 ± 1^b*	***0.70***	9 ± 2^a	6 ± 2^a	***1.53***
		3-ring PAHs	44 ± 6^a	48 ± 7^a	***0.92***	22 ± 2^a	25 ± 4^a	***0.87***	18 ± 4^a	14 ± 2^a	***1.20***
		4-ring PAHs	14 ± 2^a	15 ± 1^a	***0.90***	6 ± 1^a	8 ± 2^a	***0.72***	4 ± 1^a	3 ± 1^a	***1.20***
		8 PAHs	82 ± 6^a	94 ± 7^a	***0.86***	37 ± 2^a	48 ± 6^a	***0.79***	31 ± 5^b	24 ± 4^a	***1.27***

Italicized letters "*a*" and "*b*" express significant differences between groups ($p < 0.05$)

B detected in BC, *X* detected in XAD-2

rates. This was achieved despite differences in trapping media but when total volumes were similar due to minimal losses of gaseous PAHs during the sampling process. For example, Aretaki et al. (2024) employed a flow rate of 4 L/min for gaseous PAH sampling via solid-phase extraction (SPE) with ISOLUTE ENV +, a polystyrene-based adsorbent, over an 8-h period, resulting in a total sampled volume of 1.92 m^3. Additionally, all the sampling methods for gaseous PAHs using low-flow pumps listed in Table 2 were designed to trap 2-ring PAHs, except for the method utilized by Jin et al. (2014), which did not focus on these compounds. This outcome contrasts with the use of high-volume active air samplers, such as those used by Albinet et al. (2007) and Lee et al. (2023), which failed to adequately detect or capture 2-ring PAHs. Moreover, the recovery values of PAHs were often estimated for the extraction process after sampling, although a potential loss of gaseous PAHs during the sampling period itself could have occurred.

Sampling duration

A long sampling period is preferable as it enhances analytical detection. However, the sample matrix can affect the GC–MS system, particularly at the active sites (i.e., silanol groups and metal ions) on the surface of the stationary phase of the GC column. This could lead to decreases in the loss of susceptible analytes due to adsorption or degradation on these active sites (Anastassiades et al. 2003; Hajšlová and ZrostlíKová 2003). Moreover, a negative effect may have occurred as a secondary consequence of the breakthrough volume, the volume of the sample pumped through the adsorbent without retaining the analytes, which could have easily taken place in our study, especially with volatile compounds like gaseous PAHs. Therefore, a shorter sampling duration is more suitable for minimizing analyte losses. According to Wauters et al. (2008), the sampling volume for environmental trace analysis of a broad spectrum of persistent organic pollutants (POPs), including PAHs, in ambient air should be small, as it would limit the detection of concentrations that are as low as sub-nanogram per cubic meter. Based on the study conducted by Lee et al. (2003), which investigated the retention of vapor-phase PAHs using XAD adsorbents, the specific retention volumes (*Vg*), defined as the volume of gas required to elute each compound at 20 °C for XAD-2, were 245, 222, 373, 637, 486, 1089, and 834 m^3/g for ACY, ACE, FLR, PHE, Ant, FLT, and PYR, respectively. Furthermore, their results indicated that the ratio of *Vg* at 20 °C to *Vg* at 40 °C for these compounds was 4.5, 3.4, 3.8, 3.9, 3.1, 3.6, and 2.7 times, respectively. These findings indicate that the mass of PAHs adsorbed onto the XAD resin increased along with higher V_g values. Consequently, higher recoveries of volatile PAHs were observed at lower sampling temperatures (Chuang et al. 1987; Lee et al. 2023). In our study, the sampling temperature was set below 10 °C, which may imply a higher *Vg* for biochar when compared with ambient temperatures and lead to reduced

Table 2 Examples of gaseous sampling methods for gaseous PAHs in ambient air around the world

Order	No. of ring PAH	Sampling technique	Sorbent media	Flow rate		Time	Total volume	Reference
				(L/min)	m^3/h	(h)	(m^3)	
1	2–4	Low flow active air sampling pump	Biochar	4.00	0.24	2	0.48	This study
2	2–4	Low-volume active air sampling	Aqueous medium (H_2O: C_2H_3N (95:5 V/V) with a surfactant (CTAB at 10^{-4} mol/L and NaCl (10^{-2} mol/L)	1.67	0.10	6	0.60	Portet-Koltalo et al. 2007
3	2–6	Gilair 3 personal air sampling pump	PDMS/Tenax TA	0.10	0.006	24	0.144	Wauters et al.2008
4	2–6	GSA SG350	PDMS/Tenax TA	0.333	0.01998	24	0.48	Lazarov et al. 2013
5	3–6	Low-volume active air sampling	Dichloromethane + ice/salt water (~0 °C)	2.00	0.12	2	0.24	Jin et al. 2014
6	2–6	Sibata MP300	Carbopack C	2.00	0.12	12	1.44	Kim Oanh et al. 2000
7	2–6	Low-volume pump	ISOLUTE ENV + (polystyrene)	4.00	0.24	8	1.92	Aretaki et al. 2024
8	3–7	High-volume active air sampling	PUF	500	30	12	360	Albinet et al. 2007
9	3–7	High-volume active air sampling	PUF + XAD-2	500	30	24	720	Lee et al. 2023

*H_2O water, C_2H_3N acetonitrile, *CTAB* cetyltrimethylammonium bromide, *NaCl* sodium chloride

losses of gaseous PAHs. Given that the specific surface area of BC500 was 98.32 m^2/g and approximately 3.5 times lower than that of XAD-2, which had a surface area of 346.6 m^2/g, a rough calculation would suggest that the sampling volume for the BC500 sampling tube should not exceed 70 m^3 based on the *Vg* value for ACY. Although this estimation has not been fully corrected, it provides a useful indication of the estimation of breakthrough volume or sampling volume for gaseous PAHs of pure biochar. For the purposes of testing this new method, several sampling durations (1, 2, 3, and 4 h) at a flow rate of 4 L/min were investigated. The corresponding volumes sampled were 0.240, 0.480, 0.720, and 0.960 m^3, respectively, which were determined to be lower than our rough calculations. This would suggest that a lower breakthrough volume may occur with biochar during the sampling process. The concentration ratios of gaseous PAHs ranged from 0.70 to 1.53 for 2-ring PAHs, 0.87 to 1.20 for 3-ring PAHs, 0.72 to 1.20 for 4-ring PAHs, and 0.79 to 1.27 for 8-PAHs, based on a comparison of detected values recorded during the two sampling periods. No significant differences were observed in the ratios when comparing 1-h and 4-h intervals for each PAH ring. This was true except for the total 8-PAHs recorded between 3 and 4 h, where a significant difference was detected. The results suggest that the reversible interaction between the adsorption and desorption processes of gaseous PAHs and biochar may reach equilibrium within 3 h. Initially, the adsorption rate was high due to the full exposure of the biochar surface. As adsorption progresses, the rate gradually decreases as more of the surface becomes covered by gaseous molecules, while the desorption rate increases as PAH molecules escape from the biochar surface. Equilibrium is reached when adsorption and desorption rates equalize, which has been estimated to occur within 3 h for biochar and gaseous PAHs in ambient air. Beyond this point, equilibrium shifts toward higher desorption than adsorption, which was possibly due to limitations in binding energies and saturation capacity. Additionally, the decrease in adsorption capacity for gaseous PAHs may have been influenced by the occurrence of moisture breakthroughs from the moisture trap, as indicated by a color change in the silica gel from blue to purple with pink hues at the 4-h sampling mark. In contrast, the silica gel remained blue for 3 h, suggesting effective moisture retention up to this point. Therefore, this issue might have an effect of losing gaseous PAHs during sampling, which influenced our calculation of the sampling volume.

Sampling temperature

A major problem that can affect gaseous sampling is the high loss of analytes. Temperature is a major factor influencing the spontaneous adsorption process on the adsorbent. In general, gas adsorption takes place when the intermolecular forces between solid–gas molecules are stronger than those between the gas–gas molecules. Consequently, the resulting degree of adsorption is similar to that of condensation, which is carried out by the liberation of heat (Erkey 2011):

$$\Delta G^\circ = \Delta H^\circ - T\Delta S^\circ \tag{5}$$

where ΔG° represents the change in Gibbs free energy; ΔH° represents the change in enthalpy; ΔS° represents the change in entropy, and T represents temperature. In the adsorption process, ΔG° is negative for the spontaneous process, while ΔS° is also necessarily negative because the adsorbed state is more ordered than the unadsorbed state. Consequently, ΔH° is always negative (as an exothermic reaction). For this reason, several studies have reported that the amounts of PAH on the adsorbents decreased along with an increase in temperature (Lamichhane et al. 2016; Srogi 2007; Xu et al. 2019). Moreover, the effect of temperature on the adsorption equilibrium is indicative of the degree of adsorption strength (Piatt et al. 1996; Jia et al. 2010). Based on the Van't Hoff equation, we can establish a formula that relates temperature change to the change in the equilibrium constant of a chemical reaction:

$$\frac{dlnK}{dT} = \frac{\Delta H^\circ}{RT^2} \tag{6}$$

where $\frac{dlnK}{dT}$ is the rate of change of the natural logarithm of the equilibrium constant with respect to temperature, ΔH° is the adsorption enthalpy, R is the gas constant, and T is the absolute temperature. The increase or decrease of K along with temperature relates to the positive or negative degree of adsorption enthalpy of the process. This is determined when values are applied to two temperatures, T_1 and T_2, with equilibrium constants K_1 and K_2, respectively. The Van't Hoff equation establishes an integration formula as follows:

$$ln\frac{K2}{K1} = \frac{-\Delta H^\circ}{R}[\frac{1}{T2} - \frac{1}{T1}] \tag{7}$$

The expression of K is a very sensitive function of temperature, wherein the exponential equation provides the temperature dependence of the equilibrium constant observed as follows:

$$K = e^{-\Delta G^\circ/RT} \tag{8}$$

Using Eqs. (5) and (8), we can establish the following:

$$K = e^{-\Delta H^\circ/RT} e^{\Delta S^\circ/R} \tag{9}$$

We can then establish the natural log of both sides:

$$lnK = -\frac{\Delta H^\circ}{R}\frac{1}{T} + \frac{\Delta S^\circ}{R} \tag{10}$$

Accordingly, we know that Eq. (10) is indicative of a straight line ($y = mx + c$), which can be plotted as ln K vs

$1/T$. Several studies have found that the $\Delta H°$ values of PAHs adsorbed on the adsorbent were observed to be negative (He et al. 1995; Hiller et al. 2008; Huang and Weber 1997; Wang et al. 2011). Therefore, the slope will be positive with a positive intercept. This would imply that the exothermic reaction would consequently indicate that the equilibrium constant would decrease along with increasing temperatures. All equations can contribute to determining that the adsorption was inversely dependent upon temperature. Moreover, K_{OA} and K_p were also employed to describe the effect of temperature on adsorption for gaseous PAHs adsorbed on BC. The octanol–air partition coefficient (K_{OA}) is an important indicator of chemical partitioning between the atmosphere and the organic phases of the environment such as soil, vegetation, and the organic components of aerosols (Shoeib and Harner 2002; Parnis et al. 2015). It can also be applied to describe the adsorption and desorption processes between the gaseous and particulate phases of semi-volatile organic compounds (SVOCs) (Ancelet et al. 2011; Liu et al. 2013) including phthalates, polybrominated diphenyl ethers (PBDEs), and polycyclic aromatic hydrocarbons (PAHs). In the absence of data, K_{OA} can be estimated using the octanol–water partition coefficient (K_{OW}) and Henry's law constant (H) as follows:

$$K_{OA} = \frac{K_{OW} xRT}{H} \tag{11}$$

where R is the ideal gas constant (8.314 J/mol. K) and T is an absolute temperature (K).

$$K_{OA} = \frac{K_{OW}}{K_{AW}} \tag{12}$$

$$K_{OA} = \frac{Conc.inoctanol/Conc.inwater}{Conc.inair/Conc.inwater} \tag{13}$$

$$K_{OA} = \frac{conc.inoctanol}{conc.inair} \tag{14}$$

The octanol–air partition coefficient can be expressed as

$$K_{OA} = \frac{S°}{\frac{p°}{RT}} \tag{15}$$

$$\log p° = \frac{-\Delta H_{sub}}{2.303RT} + b_{sub} \tag{16}$$

$$\log s° = \frac{-\Delta H_{sol}}{2.303RT} + b_{sol} \tag{17}$$

where the ΔH and b variables are considered temperature independent. The enthalpy of sublimation (ΔH_{sub}) and the enthalpy of dissolution in octanol (ΔH_{sol}) are expressed in J/mol. The enthalpy of transitioning from an octanol solution to air is denoted as $\Delta_O^A H$. The temperature dependence of K_{OA} can be determined by the following equation:

$$\log K_{OA} = \frac{(\Delta H_{sub} - \Delta H_{sol})}{2.303RT} - b_{sub} - b_{sol} + \log RT \tag{18}$$

where K'_{OA} has units of concentration/pressure, $\Delta_o{}^A H = \Delta H_{sub} - \Delta H_{sol}$ and the intercept $(b_{sol} - b_{sub})$ is a constant.

Moreover, the partitioning of SVOCs between the gaseous and particulate phases at equilibrium was estimated using the SVOC particle/gas partition coefficient (K_p), which was determined based on the saturation vapor pressure of the pure sub-cooled liquid, p_L^o (Weschler et al. 2008). The equilibrium of concentrations between the gaseous and particle phases of SVOCs is defined as

$$C_g = \frac{(\frac{F}{TSP})}{K_p} \tag{19}$$

where F (ng/m^3) and C_g (ng/m^3) are the equilibrium concentrations of the compounds in the particulate phase and the gas phase, respectively, TSP (μg/m^3) is the total concentration of suspended airborne particles, and K_p is the particle/gas partition coefficient (m^3/μg).

Pankow (1994) determined the particle/gas partition coefficient (K_p) (m^3/μg) based on the absorptive process:

$$K_p = \frac{f_{om} RT}{MW_{om} \gamma p^0_{L,T} 10^6} \tag{20}$$

where f_{om} is the mass fraction of organic compounds in the particle phase, R is the gas constant (8.314 J/mol K), T is the absolute temperature (K), MW_{om} is the mean molecular mass of the organic matter phase (g/mol), γ is the activity coefficient of the compound in the organic matter on a mole fraction basis, and $p^0{}_L$ is the vapor pressure of the pure SOC (subcooled liquid in the case of solids) (Pa).

The phase transition of a single constituent between the liquid phase and the gas-phase can be characterized by the Clausius-Clapeyron relationship:

$$\frac{dp^0_{L,T}}{dT} = \frac{\Delta H}{T\Delta V} \tag{21}$$

where ΔH represents the phase change enthalpy (J/mol) and ΔV represents the volume change of the constituent during the phase change (m^3/mol). The phase change enthalpies for SVOCs were obtained from the previously published literature of Acree and Chickos (2010).

Based on the assumptions that (i) the change in SVOC volume in the liquid phase is small compared to the change

in the gas phase, (ii) the gas phase containing SVOCs behaves as an ideal gas, and (iii) the variance in the phase change enthalpy for SVOCs is negligible at ambient temperature, the change in the volume of the SVOC during the phase transition can be represented as follows:

$$\Delta V = \frac{RT}{p^0_{L,T}} \tag{22}$$

Combining Eqs. (21) and (22),

$$\frac{dp^0_{L,T}}{dT} = \frac{p^0_{L,T}\Delta H}{RT^2} \tag{23}$$

Therefore,

$$\frac{p^0_{L,2}}{p^0_{L,1}} = e^{\frac{\Delta H}{R}\left(\frac{1}{T1}-\frac{1}{T2}\right)} \tag{24}$$

Accordingly, we can assume that the variation in the activity coefficient of SVOCs in particles is minimal across various room temperatures.

$$K_{p2} = K_{p1}\frac{T2}{T1}e^{\frac{\Delta H}{R}\left(\frac{1}{T2}-\frac{1}{T1}\right)} \tag{25}$$

And further establish

$$\log K_{p2} = \frac{\Delta H}{2.303R}\left(\frac{1}{T2}-\frac{1}{T1}\right) + \log\frac{T2}{T1} + \log K_{p1} \tag{26}$$

As per Eq. (24), log $K_{p,T}$ is a temperature-dependent function that varies with log T and $\Delta H/(2.303RT)$. We can then arrive at the following equation:

$$f(T) = \frac{log\frac{T2}{T1}}{\frac{1}{T2}-\frac{1}{T1}} \tag{27}$$

$$f(T) = \frac{\Delta H}{2.303R} \tag{28}$$

If $|f(T)| << |f(\Delta H)|$, then $f(T)$ is negligible compared to $f(\Delta H)$. This suggests that when ΔH is high and the temperature varies within a narrow range, Eq. (26) can be reduced to

$$\frac{\log K_{p2} - log K_{p1}}{\frac{1}{T2}-\frac{1}{T1}} \approx \frac{\Delta H}{2.303R} \tag{29}$$

Therefore,

$$\log K_{p,T} = \frac{A}{T} + B \tag{30}$$

where $A \approx \Delta H/(2.303R)$ and B is a constant that varies among each compound. Equation (30) represents the theoretical relationship between K_p and temperature based on the adsorptive mechanism (Schwarzenbach et al. 2003). This relationship between log K_p and $1/T$ has been confirmed in previous studies (Pankow 1987; Boethling and Mackay 2000; Finlayson-Pitts and Pitts 2000; Seinfeld and Pandis 2006; Wei et al. 2016). Therefore, as temperature increases, K_p values decrease, indicating an influence on C_g values or the concentration of compounds in the gaseous phase.

To reduce this loss, two ranges of temperatures, including low temperature (≤ 10 °C) and ambient air (30–45 °C), were applied to the sampling tube containers for testing. Initially, a commercial adsorbent (i.e., XAD-2) was used to verify this hypothesis. In each sampling batch, two sets of sampling tubes packed with 150 mg of XAD-2 were connected and placed into the sampling box. Air samples were drawn at a flow rate of 2 L/min for 2 h. The results presented in Table 3 show that only 2-ring PAHs and 8-PAHs exhibited statistically significant differences. For hydrophobic organic compounds, such as PAHs, the primary adsorption mechanism is known as "hydrophobic sorption" which refers to the combined effect of London dispersion (van der Waals) forces. These molecular interactions increase with the size and flexibility of the adsorbate molecule, enhancing its ability to conform to the adsorbent surface. According to Wang et al. (2011), the enthalpy of adsorption becomes increasingly negative with larger PAHs, indicating stronger van der Waals interactions. Similarly, Petrucci et al. (2007) explained that higher molecular weight compounds tend to exhibit stronger van der Waals forces due to greater polarizability and larger electron clouds, resulting in increased intermolecular attractions. It is understood that 2-ring PAHs, such as NAP, are the smallest and most highly volatile molecules that predominantly exist in the gaseous phase. Consequently, their adsorption to surfaces is relatively low when compared with larger PAHs, making them more susceptible to losses during the sampling process. These findings are consistent with those of Hiller et al. (2008), who reported that NAP adsorption on various sorbents decreased along with increasing temperatures. This explains why NAP concentrations were the only significantly different values observed, along with 8-PAHs, which are typically the most abundant PAHs in ambient air. BC was subsequently tested under the same conditions. No significant differences were observed in the concentrations of 4-ring PAHs. However, differences between the two adsorbents were noted and were likely due to their specific properties. For example, XAD-2 possesses a chemically homogeneous and nonionic structure, as well as unique macroreticular porosity, which makes it effective for adsorbing organic pollutants (dos Reis et al. 2013; Sigma-Aldrich Co. 1997). In contrast, BC has a heterogeneous surface and a relatively low surface area, as has been previously described in sections

of physicochemical characterization. Nevertheless, both adsorbents demonstrated that low sampling temperatures can significantly reduce the loss of volatile compounds, thereby enhancing the efficiency of gaseous PAHs.

Amount of BC used

Various publications (Matovic 2011; Mohan et al. 2014; Qadeer et al. 2014; Zhang et al. 2013) have demonstrated the effective use of biochar (BC) for soil conditioning, remediation, and carbon sequestration of both organic and inorganic compounds including polycyclic aromatic hydrocarbons (PAHs). However, the use of BC as an adsorbent for the collection of gaseous PAHs has not been extensively explored. This is likely because adsorption efficiency depends upon the physicochemical properties of both the adsorbent and the adsorbate. It is also important to note that BC can be influenced by the composition of raw materials during its heat treatment process, which, in turn, can affect its properties (Lian et al. 2014).

In our study, we did not test the adsorption capacity of BC in a controlled laboratory environment using a closed chamber. Instead, we conducted gaseous PAH sampling under real ambient conditions. For the purposes of comparison, we used commercial XAD-2 as a reference adsorbent to evaluate the sampling efficiency of gaseous PAHs using our lab-made BC. The results indicated that the efficiency of our developed BC was not significantly different from that of XAD-2 when used in the developed gaseous PAH sampling device. However, sampling gaseous PAHs can present challenges, particularly in terms of vaporization loss during the sampling process. To mitigate this issue, the use of sandwiched adsorbents or sample train sampling has been recommended to improve the potential for gaseous PAH sampling. During our sampling process, a pressure drop in the vacuum pump was observed, which led us to compare different amounts of BC, at 150 mg and 250 mg, to assess their efficiency in collecting gaseous PAHs. This comparison was made prior to finalizing the optimal amount of BC for use in the developed gaseous PAH sampling device.

Table 3 shows the detected PAHs adsorbed on 150 mg and 250 mg of biochar and the ratio of concentrations between the two amounts (150 mg/250 mg). It was found that there were no significant differences between the two amounts of BC used for each ring and 8-PAHs. Based on these findings, both amounts of BC could be used for low concentrations of gaseous PAH sampling in ambient air. However, 250 mg was chosen because it may help reduce any losses associated with breakthrough volume if high concentrations of PAHs are found in the ambient air.

Due to the limitations of chamber testing in the laboratory, an indirect comparison method was used to assess the efficiency of biochar (BC) in field validations relative to XAD-2, while employing a spiking approach. In this method, 100 ng of each gaseous PAH (equivalent to 208 ng/m^3) was spiked onto the adsorbents inside the sampling tubes, which included both BC (150 mg and 250 mg) and XAD-2 (150 mg). These spiked samples were then aged overnight in a refrigerator to ensure complete adsorption of the PAHs onto the adsorbents. Subsequently, they were used to sample gaseous PAHs in the field, and the samples were analyzed using the previously described method. The recovery values for 2–4 ring PAHs from all adsorbents were found to be quite similar. For BC, the recovery rates were 88–96% for the 150 mg sample, 90–103% for the 250 mg sample, and 85–104% for XAD-2. These results suggest that both the 150 mg and 250 mg BC samples, as well as XAD-2, demonstrated comparable degrees of efficiency for sampling gaseous PAHs. This confirms that the amounts of adsorbent used in this study were suitable and acceptable for gaseous PAH sampling in ambient air, providing confidence in the reliability of BC as an adsorbent for this purpose.

Moreover, when compared with other studies using low-volume active air sampling for gaseous PAHs, the amount of adsorbent used in our study was similar to that which was used in other research work. For example, Wauters et al. (2008) used 120 mg of PDMS and 60 mg of Tenax TA, while Aretaki et al. (2024) used 200 mg of polystyrene to develop a sampling device for gaseous PAHs. However, in our research work, we used a higher amount of biochar due to its lower physical properties when compared with the commercial adsorbents used in those other studies. The similar amounts of adsorbent used across all the developed sampling devices likely served the same purpose, which was to prevent pressure drops during sampling. This is because the low-flow pump used to collect the air sample had a lower capacity to handle large pressure drops in the sampling media when compared with high-volume active air sampling. Therefore, achieving the desired flow rate over the sampling period was a simpler task for the low-flow pump (McCammon and Woebkenberg 2016).

Consecutive sampling tube

In previous studies, commercial adsorbents, such as PUF and XAD resins, were used individually for sampling gaseous PAHs (Pankow 1988; Zaranski et al. 1991). However, these adsorbents were not proven to be artifact-free (Temime et al. 2002). A significant consideration in active sampling is the potential loss of gaseous PAHs, which may be adsorbed by downstream sampling media. To address this issue, a sampling device was developed using a sandwiched configuration of sampling media to achieve higher collection efficiency, particularly for low molecular weight PAHs such as naphthalene (NAP). For example, the use of PUF/XAD-4/PUF (Xie et al. 2014) and PUF/XAD-2 (Xu et al.

Table 3 Effect of sampling temperature, amount and number sampling tube on the adsorbent efficiency for gaseous PAHs, and comparison of the efficiency of XAD-2 and BC based on the gaseous PAH device in ambient air

		Detected gaseous PAHs (ng/m^3)					
		Mean ± SD (n=3)					
Parameter	Sampling temperature	Compound	XAD-2		*Ratio (B/X)*	BC		***Ratio (B/X)***
			Ambient temp (30-45 °C)	Low temp (≤10 °C)		Ambient temp (30-45 °C)	Low temp (≤10 °C)	
		2-ring PAHs	15 ± 5^a	32 ± 4^b	***0.46***	16 ± 3^a	36 ± 3^b	***0.45***
		3-ring PAHs	26 ± 2^a	29 ± 2^a	***0.92***	32 ± 1^a	58 ± 3^b	***0.56***
		4-ring PAHs	7 ± 1^a	10 ± 1^a	***0.68***	9 ± 4^a	18 ± 6^a	***0.57***
		8–PAHs	48 ± 5^a	71 ± 5^b	***0.68***	58 ± 11^a	112 ± 11^b	***0.52***
	Amount and number of sampling tube	Compound	Single tube of BC		Ratio	Two tubes of BC	Single tube of BC	Ratio
			150 mg	250 mg	(150/250)	250 mg + 150 mg	250 mg	(250 +150)/250)
		2-ring PAHs	32 ± 14^a	29 ± 12^a	*1.10*	70 ± 16^b	56 ± 15^a	*1.27*
		3-ring PAHs	41 ± 15^a	42 ± 22^a	*0.78*	75 ± 1^b	55 ± 3^a	*1.07*
		4-ring PAHs	19 ± 10^a	18 ± 8^a	*1.10*	24 ± 4^a	15 ± 0.2^a	*1.57*
		8–PAHs	101 ± 37^a	100 ± 39^a	*1.02*	189 ± 16^b	140 ± 12^a	*1.35*
		Compound	Day 1		Ratio (X/B)	Day 2		Ratio (X/B)	Day 3		Ratio (X/B)
			X	B		X	B		X	B	
Session	Morning (9-11 am)	2-ring PAHs	90	99	*0.91*	58	65	0.89	145	122	*1.19*
		3-ring PAHs	68	66	*1.02*	42	41	1.01	59	55	*1.08*
		4-ring PAHs	20	19	*1.06*	16	16	0.99	12	13	*0.95*
		8–PAHs	178	184	*0.97*	116	122	0.95	217	190	*1.14*
	Afternoon (2-4 pm)	2-ring PAHs	79	91	*0.87*	29	39	0.74	105	91	*1.15*
		3-ring PAHs	63	57	*1.11*	71	71	1.00	71	72	*0.99*
		4-ring PAHs	13	12	*1.09*	27	30	0.89	18	14	*1.25*
		8–PAHs	155	158	*0.98*	126	140	0.90	193	177	*1.10*

Italic alphabets "*a*" and "*b*" express significant difference between groups ($p < 0.05$)

A detected from ambient temperature, *L* detected from low temperature,*150* detected from 150 mg, *250* detected from 250 mg, *X* detected in XAD-2, *B* detected in BC

2012; Singh et al. 2023) has been found to facilitate higher efficiency when compared with using a single adsorbent alone (Zaranski et al. 1991; Lee et al. 2004). Notably, this design helps prevent compound loss during both sampling and extraction processes (Jia et al. 2020).

In this study, we examined the efficiency of gaseous PAH sampling by comparing the use of one versus two sampling tubes to determine whether this configuration could improve collection efficiency. Initially, two connected sampling tubes (each containing 250 mg of BC500) were used for air sampling at a flow rate of 4 L/min for 2 h. However, a pressure drop was observed before the sampling period was completed. A second test was then conducted under the same conditions, but with a reduced amount of BC500 in the second tube (250 mg in the first tube and 150 mg in the second).

As is shown in Table 3, gaseous PAHs were detected in both the first and second sampling tubes for 2-ring, 3-ring, and 4-ring PAHs. These results indicate that the use of only

one sampling tube with biochar was insufficient for collecting gaseous PAHs from ambient air. This finding aligns with studies that used commercial sorbents for gaseous PAH sampling, such as PUF/XAD-4/PUF (Xie et al. 2014) and PUF/XAD-2 (Lee et al. 2024; Singh et al. 2023; Xu et al. 2012), in high-volume active air sampling, or PDMS/Tenax TA (Lazarov et al.; Wauters et al. 2008) in low-volume active air sampling.

The outcomes of our research have also indicated that low temperatures could play an important role in gaseous PAH sampling in ambient air, particularly for retaining gaseous PAHs and removing moisture during the sample preparation step before analysis by GC techniques. Although the results indicate that a higher number of gaseous PAHs was found in the second sampling tube, this may have been due to the low temperature, which could have helped retain gaseous PAHs, or the limitations of the biochar's physical properties such as specific surface area and heterogeneous surface characteristics.

Overall, the method we developed for gaseous PAH sampling using two connected sampling tubes shows promise and warrants further refinement and validation. This approach offers a reliable foundation for continued monitoring and method improvement.

Validation of the developed gaseous PAH device

This investigation was conducted under the same optimum conditions that were used during the sampling method. There were two connected sampling tubes (1st: 250 mg; 2nd: 150 mg) operating under low sampling flow rates (4 L/min) and at low temperatures (≤ 10 °C) during 2-h periods of sampling.

Method for detection limit The performance of the developed gaseous PAH device was then further tested. The method detection limit (MDL) and LOQ values were calculated by 3 and 10 times the standard deviation of the field blank, respectively. The MDL values were 0.26 ng/m^3 (ACY) to 4.43 ng/m^3 (NAP), while the LOQ values ranged from 0.86 ng/m^3 (ACY) to 14.76 ng/m^3 (NAP) (Supplementary Table A.1).

Accuracy of developed gaseous PAH sampling device The recovery values of the gaseous PAHs were used to assess the accuracy of both the sampling preparation and analysis methods. To determine these recovery rates, the sampling tube containing BC500 was spiked with a mixed 8 PAH standard, with each compound being added at a concentration of 80 ng. The sample was then aged or incubated at a cooled temperature overnight to ensure complete adsorption before being used in the sampling procedure. Although the optimal configuration consisted of two connected sampling tubes (250 mg of BC in the first tube and 150 mg in the second), only the first sampling tube was spiked for recovery testing. However, upon analysis, it was found that gaseous PAHs were present in both sampling tubes. The first sampling tube yielded $70 \pm 4\%$ of the total 8-PAHs, while the second tube yielded $11 \pm 4\%$. The gaseous PAH compounds were also grouped according to their number of rings to assess their absorption by biochar. The recovery values for 2-ring, 3-ring, and 4-ring PAHs in the first sampling tube were $43 \pm 1\%$, $71 \pm 4\%$, and $84 \pm 7\%$, respectively, while those in the second tube were $15 \pm 1\%$, $10 \pm 5\%$, and $11 \pm 5\%$, respectively. To confirm the efficiency of the developed gaseous PAH sampling device, a mixed PAH standard was spiked onto 150 mg of XAD-2, which was then packed into a sampling tube before analysis using the same procedure. The PAH recovery values were found to be $79 \pm 3\%$ for 8-PAHs, $54 \pm 2\%$ for 2-ring PAHs, $76 \pm 3\%$ for 3-ring PAHs, and $100 \pm 6\%$ for 4-ring PAHs (Supplementary Fig. A2). Additionally, after extraction, neither biochar nor XAD-2 adsorbents could be reused, as they were found to stick to the syringe filter that was used to obtain filter extracts from both adsorbents.

According to Jia et al. (2020), the acceptable recovery range for field validation using standard compounds, which assess recovery during sample collection, handling, and analysis, typically falls between 60 and 120%. In their study, the sampling media for gaseous PAHs consisted of sandwiched sorbents containing polyurethane foam (PUF)/XAD/PUF, which were deployed in the field. Their results reflected recovery values of 72.8% for 3-ring PAHs and 89.2% for 4-ring PAHs. Based on these criteria, the recovery results from the developed gaseous PAH sampling device fall within the acceptable range for PAH sampling, as has been explained above.

Application of the developed gaseous PAH device for air sampling

After the gaseous PAH sampling device was completely optimized, it was then used for air sampling in the real environment. The sampling efficiency of the BC500 sampling tube was compared with that of the commercial XAD-2. A single tube packed with 150 mg XAD-2 and two connected sampling tubes containing BC500 (250 mg + 150 mg) were set up for air sampling over the same period of time. They were employed on the same day in both the morning and afternoon sessions, as well as on consecutive days. The gaseous PAHs that were detected were present in the parallel sampling devices, as shown in Table 3. The PAH concentrations collected by the two types of adsorbents used in the sampling device were not significantly different. The PAH ratio values (*X*/*B*) were within the ranges of 0.74–1.19

(2-ring PAHs), 0.99–1.11 (3-ring PAHs), 0.95–1.25 (4-ring PAHs), and 0.97–1.14 (Σ 8-PAHs). The PAH concentrations detected by BC and XAD may vary due to various conditions. In this case, a higher level of NAP concentrations was detected in the BC adsorbent than in XAD, although the opposite result was observed on the last day. The reason for this is because NAP is a highly volatile compound, and it can cause substantial fluctuations during the sampling and analysis processes.

The percentage ratios of gaseous PAHs collected by BC500 were also compared between the morning and afternoon sessions. It was found that the 2-ring PAHs were dominant during both sampling times (57% and 46%, respectively) (Supplementary Fig. A3). These ratios varied due to changes in meteorological conditions (such as temperature and humidity) and the presence of some pollutants (such as nitrogen oxide and ozone), which influenced the reaction with the gaseous PAHs (Liu et al. 2014; Martins et al. 2013).

Based on these results, it can be concluded that the sampling device was effective in the detection of gaseous PAHs in the field. Furthermore, the findings of this research study would indicate that the advantage of field validations would also reduce the problem of interference during optimization. This could reduce the problem of a real sample analysis, which would differ from the outcomes of a laboratory validation.

However, only a low recovery of NAP (58%) was obtained from the standard spiking test. As previously mentioned, it is important to note that the high volatility of this compound is a drawback in the overall determination, especially during the hot dry season in Northern Thailand. This outcome can be confirmed by US EPA TO-13A (US EPA 1999), in which polyurethane foam (PUF) was used and only 35% sampling efficiency of NAP was obtained. Strandberg et al. (2022) also reported a low recovery of NAP (50%), while many other publications avoided reporting these compounds (Jin et al. 2014; Lazarov et al. 2013; Magnusson et al. 2016; Sabino et al. 2016; Strandberg et al. 2022).

When comparing the results of Kongpran et al. (2021), PAHs were collected throughout northern Thailand in Chiang Rai, Mae Hong Son, Nan, Lampang, Lampang, and Tak. However, in Chiang Mai, both gaseous PAHs and particulate PAHs were collected during 24-h sampling intervals. It was found that the distribution of 3-rings was as follows: (50.67%) > 2-ring PAHs (47.65%) > 4-ring PAHs (1.68%). Notably, the order of distribution was reversed in our research study. This might have been the result of employing a different sampling method. For example, only XAD-2 adsorbent was used for gaseous PAHs at a flow rate of 10 L/min under high temperatures of ambient air, for which the recovery of all steps employed for this determination was not expected to be used in the extraction method. However, the results were confirmed by the results of Wauters et al. (2008), who compared the gaseous PAHs between high volume active air sampling (PUF) and developed adsorbents (PDMS/Tenax TA) with a low flow pump. Accordingly, it was found that the ratio of 2-ring PAHs, 3-ring PAHs, and 4-ring PAHs was 34.98, 1.69, and 1.37 times, respectively. Moreover, our results revealed that the order of gaseous PAHs was similar to that reported by Wauters et al. (2008) as follows: 2-ring PAHs (72.88%) > 3-ring PAHs (22.49%) > 4-ring PAHs (4.63%), respectively.

Implications

In general, XAD resins are among the most widely used adsorbents for sampling gaseous PAHs due to their high adsorption efficiency. However, they are relatively expensive and non-regenerable, making them a consumable material. These limitations highlight the need for a more cost-effective alternative in the development of practical sampling methods. Spent coffee grounds (SCGs), which are renewable bioresources derived from coffee production, are inevitably generated as waste during the coffee extraction process and offer potential as an alternative adsorbent. Based on recovery values, comparative analysis with commercially available XAD-2 showed that SCG-derived biochar (BC) exhibits good adsorption efficiency toward 8 PAHs, even though it may possess lower physicochemical properties, such as specific surface area, when compared with XAD-2. Ultimately, applicability and cost-effectiveness are key factors in selecting a suitable adsorbent for gaseous compound sampling. This study indicates that BC is a promising alternative adsorbent for monitoring gaseous PAHs in ambient air and can compete with commercial XAD-2 in terms of sampling efficiency. In terms of production cost, BC derived from biomass is significantly cheaper. According to González-Pernas et al. (2022), the average price of BC is approximately €0.800/kg, which is only about 0.18% of the cost of XAD-2 (€444/kg, Sigma-Aldrich Co. 2022). We estimate the cost of BC used for one sampling (250 mg + 150 mg) to be just €0.00032. Therefore, the cost of BC is roughly 200 times lower than that of commercial XAD-2. However, it is important to note that commercial-scale BC production involves several additional steps that could increase its final cost. According to the BPT (Business Plan Templates) team (2024), operating a biochar production facility incurs various expenses that can significantly contribute to overall costs. These include raw material costs (30–50%), skilled labor (20–30%), utilities such as electricity and water (10–15%), equipment maintenance (5–10%), transportation (10–20%), packaging (5–7%), insurance and licensing fees (3–5%), marketing and sales (5–10%), and waste management (2–3%). Moreover, while the high efficiency of biochar across various applications is promising, it often requires modifications that can further increase production costs. For

example, Maneechakr and Mongkollertlop (2020) reported that modifying biochar with magnetite (Fe_3O_4) or manganese oxide (MnO_2) increased its surface area by approximately 14 times when compared with unmodified biochar. These enhancements significantly improved its adsorption capacity for trivalent chromium (Cr^{3+}) and lead (Pb^{2+}) when compared with commercial activated carbon. However, such modifications substantially increase production costs, often exceeding those of pristine biochar and even some commercial activated carbons. Overall, the device and approach developed in this research demonstrate promising potential for the future application of BC in the quantitative analysis of gaseous PAHs.

Conclusions

Gaseous polycyclic aromatic hydrocarbons (PAHs) react with other pollutants in the ambient air, forming highly hazardous chemicals that pose significant risks to both the environment and human health. To address this issue, an innovative active sampling technique has been developed for determining the concentration of these compounds in the air.

The results of this study demonstrate that biochar (BC) can effectively serve as an adsorbent for gaseous PAH sampling in ambient air. While BC has lower physical properties, such as surface area and hydrophobicity, when compared with XAD-2, the design of the sampler can significantly improve its sampling efficiency. The optimal conditions for sampling gaseous PAHs using the proposed device are as follows: (1) two connected sampling tubes, each containing 250 mg and 150 mg of BC, and kept in a container at temperatures below 10 °C; (2) a sampling flow rate of ≤ 4 L/min; and (3) a sampling duration of 1–3 h.

The recovery values for the 8-PAHs obtained from BC did not significantly differ from those obtained using 150 mg of XAD-2 as the reference adsorbent in the sampling tube. This method demonstrated excellent performance, with high sensitivity in estimating the concentration of gaseous PAHs. The simplicity, low cost, and positive performance of the proposed sampler make it a promising tool for monitoring a wide range of gaseous PAHs in ambient air.

However, the use of BC is associated with some limitations due to its properties. BC typically has a heterogeneous surface with both hydrophobic and hydrophilic functional groups. The hydrophilic portions of BC can retain moisture, which may interfere with the passage of gaseous PAHs, especially during longer sampling periods. This issue may be mitigated by modifying the surface area of BC with the intention of enhancing its long time of adsorption efficiency in future studies.

Furthermore, the sampling pump must be compatible with both the sampling duration and the sampling device in order to avoid certain problematic issues such as pressure drop and pump overheating, which could affect the accuracy of the results.

Supplementary Information The online version contains supplementary material available at https://doi.org/10.1007/s11356-025-36682-z.

Author contribution Wittaya Tala: conceptualization, methodology, validation, formal analysis, investigation, data curation, writing the original draft, and visualization. Suparin Chaiklangmuang: supervision and resources. Somporn Chantara: conceptualization, resources, writing—review and editing, visualization, and supervision. All authors have read and approved of the final version of this manuscript.

Funding This research work was partially supported by Chiang Mai University (CMU), Thailand. Also, special thanks are extended to the Fuel and Fuel Technology Laboratory, Department of Industrial Chemistry, Faculty of Science, Chiang Mai University, for facilitating production of BC.

Data availability The datasets used and/or analyzed during the current study are available from the corresponding author upon reasonable request.

Declarations

Ethics approval Not applicable.

Consent to participate Not applicable.

Consent for publication Not applicable.

Competing interests The authors declare no competing interests.

References

Abdel-Shafy HI, Mansour MSM (2016) A review on polycyclic aromatic hydrocarbons: source, environmental impact, effect on human health and remediation. Egypt J Pet 25:107–123. https://doi.org/10.1016/j.ejpe.2015.03.011

Acree W, Chickos JS (2010) Phase transition enthalpy measurements of organic and organometallic compounds: sublimation, vaporization and fusion enthalpies from 1880 to 2010. J Phys Chem Ref Data 39:1–942. https://doi.org/10.1063/1.3309507

Albinet A, Leoz-Garziandia E, Budzinski H, ViIlenave E (2007) Polycyclic aromatic hydrocarbons (PAHs), nitrated PAHs and oxygenated PAHs in ambient air of the Marseilles area (South of France): Concentrations and sources. Sci Total Environ 384:280–292. https://doi.org/10.1016/j.scitotenv.2007.04.028

Anastassiades M, Maštovská K, Lehotay SJ (2003) Evaluation of analyte protectants to improve gas chromatographic analysis of pesticides. J Chromatogr A 1015:163–184. https://doi.org/10.1016/S0021-9673(03)01208-1

Ancelet T, Davy PK, Trompetter WJ, Markwitz A, Weatherburn DC (2011) Carbonaceous aerosols in an urban tunnel. Atmos Environ 45:4463–4469. https://doi.org/10.1016/j.atmosenv.2011.05.032

Aretaki MA, Desmet J, Viana M, van Drooge BL (2024) Comprehensive methodology for semi-volatile organic compound determination in ambient air with emphasis on polycyclic aromatic hydrocarbons analysis by GC–MS/MS. J Chromatogr A 1730:465086. https://doi.org/10.1016/j.chroma.2024.465086

Bandowe BAM, Meusel H (2017) Nitrated polycyclic aromatic hydrocarbons (nitro-PAHs) in the environment – a review. Sci Total Environ 581–582:237–257. https://doi.org/10.1016/J.SCITOTENV.2016.12.115

Bartkow ME, Booij K, Kennedy KE, Muller JF, Hawker DW (2005) Passive air sampling theory for semivolatile organic compounds. Chemosphere 60:170–176. https://doi.org/10.1016/j.chemosphere.2004.12.033

Boethling RS, Mackay D (2000) Handbook of property estimation methods for chemicals: environmental and health sciences. 1st edn. CRC Press (Lewis Publishers), Boca Raton, Florida

Bohlin P, Jones KC, Strandberg B (2010) Field evaluation of polyurethane foam passive air samplers to assess airborne PAHs in occupational environments. Environ Sci Technol 44:749–754. https://doi.org/10.1021/es902318g

BPT (Business Plan Templates) Team (2024) What are the main Costs of Biochar Production? https://businessplan-templates.com/blogs/running-costs/biochar-production-company. Accessed 20 Jan 2025

Cao T, Chen W, Yang T, He T, Liu Z, Meng J (2017) Surface characterization of aged biochar incubated in different types of soil. Bioresources 12:6366–6377. https://doi.org/10.15376/BIORES.12.3.6366-6377

Choi S-D, Baek S-Y, Chang Y-S (2009) Passive air sampling of persistent organic pollutants in Korea. Toxicol Environ Health Sci 1:75–82. https://doi.org/10.1007/BF03216467

Chu SN, Sands S, Tomasik MR, Lee PS, McNeill VF (2010) Ozone oxidation of surface-adsorbed polycyclic aromatic hydrocarbons: role of PAH-surface interaction. J Am Chem Soc 132:15968–15975. https://doi.org/10.1021/ja1014772

Chuang JC, Hannan SW, Wilson NK (1987) Field comparison of polyurethane foam and XAD-2 resin for air sampling for polynuclear aromatic hydrocarbons. Environ Sci Technol 21:798–804. https://doi.org/10.1021/es00162a011

Crocker M (2010) Thermochemical conversion of biomass to liquid fuels and chemicals, 1st edn. Royal Society of Chemistry Publishing, London, pp 190–219

de Oliveira Galvao MF, de Oliveira AN, Ferreira PA, Caumo S, de Castro VP, Artaxo P, de Souza HS, Roubicek DA, de Medeiros SR (2018) Biomass burning particles in the Brazilian Amazon region: mutagenic effects of nitro and oxy-PAHs and assessment of health risks. Environ Pollut 233:960–970. https://doi.org/10.1016/j.envpol.2017.09.068

dos Reis LGT, Gallart-Mateu D, Pacheco WF, Pastor A, de la Guardia M, Cassella RJ (2013) Study of passive sampling of polycyclic aromatic hydrocarbons in gas phase using Amberlite XAD resins as filling materials of semipermeable membranes. Microchem J 110:494–500. https://doi.org/10.1016/j.microc.2013.06.003

Drotikova T, Ali AM, Halse AK, Reinardy HC, Kallenborn R (2020) Polycyclic aromatic hydrocarbons (PAHs), oxy-, and nitro-PAHs in ambient air of Arctic town Longyearbyen Svalbard. Atmos Chem Phys 20:9997–10014. https://doi.org/10.5194/acp-20-9997-2020

Dumroese RK, Heiskanen J, Englund K, Tervahauta A (2011) Pelleted biochar: chemical and physical properties show potential use as a substrate in container nurseries. Biomass Bioenergy 35:2018–2027. https://doi.org/10.1016/j.biombioe.2011.01.053

Eiguren-Fernandez A, Avol EL, Thurairatnam S, Hakami M, Froines JR, Miguel AH (2007) Seasonal influence on vapor-and particle-phase polycyclic aromatic hydrocarbon concentrations in school communities located in Southern California. Aerosol Sci Technol 41:438–446. https://doi.org/10.1080/02786820701213511

El-Sayed SA, Mostafa ME (2020) Thermal pyrolysis and kinetic parameter determination of mango leaves using common and new proposed parallel kinetic models. RSC Adv 10:18160. https://doi.org/10.1039/D0RA00493F

Erkey C (2011) Supercritical fluid science and technology: Chapter 4-Thermodynamics and dynamics of adsorption of metal complexes on surfaces from supercritical solutions. Elsevier Science. O'Reilly Media, Inc

Finlayson-Pitts BJ, Pitts JN Jr (2000) Chemistry of the upper and lower atmosphere: theory, experiments and applications. Academic Press, San Diego, California

Fu P, Yi W, Bai X, Li Z, Hu S, Xiang J (2011) Effect of temperature on gas composition and char structural features of pyrolyzed agricultural residues. Bioresour Technol 102:8211–8219. https://doi.org/10.1016/j.biortech.2011.05.083

Galarneau E, Bidleman TF (2006) Modelling the temperature-induced blow-off and blow-on artefacts in filter-sorbent measurements of semivolatile substances. Atmos Environ 40:4258–4268. https://doi.org/10.1016/J.ATMOSENV.2006.04.006

Ghani WA, Mohd A, Silva G, Bachmann RT, Taufiq-Yap YH, Rashid U, Al-Muhtaseb AH (2013) Biochar production from waste rubber-wood-sawdust and its potential use in C sequestration: chemical and physical characterization. Ind Crops Prod 44:18–24. https://doi.org/10.1016/j.indcrop.2012.10.017

González-Pernas FM, Grajera-Antolín C, García-Cámara O, González-Lucas M, Martín MT, González-Egido S, Aguirre JL (2022) Effects of biochar on biointensive horticultural crops and its economic viability in the Mediterranean climate. Energies 15:3407. https://doi.org/10.3390/en15093407

Hajšlová J, ZrostlíKová J (2003) Matrix effects in (ultra) trace analysis of pesticide residues in food and biotic matrices. J Chromatogr A 1000:181–197. https://doi.org/10.1016/S0021-9673(03)00539-9

Han L, Qian L, Liu R, Chen M, Yan J, Hu Q (2017) Lead adsorption by biochar under the elevated competition of cadmium and aluminum. Sci Rep 7:1–11. https://doi.org/10.1038/s41598-017-02353-4

He Y, Yediler A, Sun T, Kettrup A (1995) Adsorption of fluoranthene on soil and lava: Effects of the organic carbon contents and temperature. Chemosphere 30:141–150. https://doi.org/10.1016/0045-6535(94)00396-C

Hiller E, Jurkovič Ľ, Bartaĺ M (2008) Effect of temperature on the distribution of polycyclic aromatic hydrocarbons in soil and sediment. Soil Water Res 3:231–240. https://doi.org/10.17221/28/2008-SWR

Huang W, Weber WJ (1997) Thermodynamic considerations in the sorption of organic contaminants by soils and sediments. 1. The isosteric heat approach and its application to model inorganic sorbents. Environ Sci Technol 31:3238–3243. https://doi.org/10.1021/es970230m

Idowu O, Semple KT, Ramadass K, O'Connor W, Hansbro P, Thavamani P (2019) Beyond the obvious: environmental health implications of polar polycyclic aromatic hydrocarbons. Environ Int 123:543–557. https://doi.org/10.1016/j.envint.2018.12.051

Jia CX, You C, Pan G (2010) Effect of temperature on the sorption and desorption of perfluorooctane sulfonate on humic acid. J Environ Sci 22:355–361. https://doi.org/10.1016/S1001-0742(09)60115-7

Jia C, Fu X, Sultana F, Akkaus C, Xue Z (2020) Final report: characterizing community exposure to atmospheric polycyclic aromatic hydrocarbons (PAHs) in the Memphis tri-state area, revision 02. https://www.epa.gov/sites/default/files/2020-01/documents/memphis_pahs_study_final_report_08.pdf. Accessed 10 Apr 2025

Jin G, Cong L, Wang H, He M, Li J, Piao X, Zhu W, Li D (2014) A simple and rapid analysis for gas-phase polycyclic aromatic hydrocarbons using an organic-solvent-based method. Atmos Environ 89:367–372. https://doi.org/10.1016/j.atmosenv.2014.01.022

Keiluweit M, Nico PS, Johnson MG, Kleber M (2010) Dynamic molecular structure of plant biomass-derived black carbon (biochar).

Environ Sci Technol 44:1247–1253. https://doi.org/10.1021/es9031419

Kim Oanh NT, Reutergårdh LB, Dung NT, Yu MH, Yao WX, Co HX (2000) Polycyclic aromatic hydrocarbons in the airborne particulate matter at a location 40 km north of Bangkok, Thailand. Atmos Environ 34:4557–4563. https://doi.org/10.1016/S1352-2310(00)00109-6

Kobayashi A, Kojima Y, Okochi H, Nagoya T (2010) Development of low volume air sampling and rapid sample preparation for the determination of atmospheric gas-phase polycyclic aromatic hydrocarbons using styrene-divinylbenzene copolymer resin adsorbent. J-STAGE 59:645–652. https://doi.org/10.2116/bunsekikagaku.59.645

Kongpran J, Kliengchuay W, Niampradit S, Sahanavin N, Siriratruengsuk W, Tantrakarnapa K (2021) The health risks of airborne polycyclic aromatic hydrocarbons (PAHs): Upper north Thailand. GeoHealth 5:e2020GH000352. https://doi.org/10.1029/2020GH000352

Kreatananchai B, Kamopas W, Kiatsiriroat T (2015) Analysis on properties of biochar from coffee ground and coffee residues from slow pyrolysis. The 14th Conference on Energy, Heat and Mass Transfer in Thermal Equipment and Processes, Chiang Mai, pp 461–468. (in Thai)

Lamichhane S, Bal Krishna KC, Sarukkalige R (2016) Polycyclic aromatic hydrocarbons (PAHs) removal by sorption: a review. Chemosphere 148:336–353. https://doi.org/10.1016/j.chemosphere.2016.01.036

Lazarov B, Swinnen R, Spruyt M, Goelen E, Stranger M, Desmet G, Wauters W (2013) Optimization steps of an innovative air sampling method for semi volatile organic compounds. Atmos Environ 79:780–786. https://doi.org/10.1016/j.atmosenv.2013.07.05

Lee JJ, Huang K-L, Yu YY, Chen MS (2004) Laboratory retention of vapor-phase PAHs using XAD adsorbents. Atmos Environ 38:6185–6193. https://doi.org/10.1016/j.atmosenv.2004.07.024

Lee JW, Kidder K, Evans BR, Paik S, Buchanan AC, Garten CT, Brown RC (2010) Characterization of biochars produced from cornstovers for soil amendment and carbon sequestration. Environ Sci Technol 44:7970–7974. https://doi.org/10.1021/es101337x

Lee Y, Cho E, Maskey S, Nguyen D, Bae H (2023) Value-added products from coffee waste: a review. Molecules 28:3562. https://doi.org/10.3390/molecules28083562

Lee Y-K, Lee J-H, Beak N-G, Kim K-C, Han J-S (2024) Seasonal and emission characteristics of PAHs in the ambient air of industrial complexes. Atmosphere 15:30. https://doi.org/10.3390/atmos15010030

Lehmann J, Joseph S (2009) Biochar for environmental management: An introduction. In: Lehmann J, Joseph S (eds) Biochar for environmental management-science and technology. Earthscan Publisher, London, pp 1–12

Lian F, Sun B, Song Z, Zhu L, Qi X, Xing B (2014) Physicochemical properties of herb-residue biochar and its sorption to ionizable antibiotic sulfamethoxazole. Chem Eng J 248:128–134. https://doi.org/10.1016/j.cej.2014.03.021

Lin SH, Hsu LY, Chou CS, Jhang JW, Wu P (2014) Carbonization process of Moso bamboo (Phyllostachys pubescens) charcoal and its governing thermodynamics. J Anal Appl Pyrolysis 107:9–16. https://doi.org/10.1016/j.jaap.2014.01.001

Liu W, Zhou R, Goh HLS, Huang S, Lu X (2010a) From waste to functional additive: toughening epoxy resin with lignin. ACS Appl Mater Interfaces 6:5810–5817. https://doi.org/10.1021/am500642n

Liu Z, Zhang FS, Wu J (2010b) Characterization and application of chars produced from pinewood pyrolysis and hydrothermal treatment. Fuel 89:510–514. https://doi.org/10.1016/j.fuel.2009.08.042

Liu C, Shi SS, Weschler CJ, Zhao B, Zhang YP (2013) Analysis of the dynamic interaction between SVOCs and airborne particles. Aerosol Sci Technol 47:125–136. https://doi.org/10.1080/02786826.2012.730163

Liu D, Xu Y, Chaemfa C, Tian C, Li J, Luo C, Zhang G (2014) Concentrations, seasonal variations, and outflow of atmospheric polycyclic aromatic hydrocarbons (PAHs) at Ningbo site, Eastern China. Atmos Pollut Res 5:203–209. https://doi.org/10.5094/APR.2014.025

Lu H, Zhu L, Chen S (2008) Pollution level, phase distribution and health risk of polycyclic aromatic hydrocarbons in indoor air at public places of Hangzhou. Environ Pollut 152:569–575. https://doi.org/10.1016/j.envpol.2007.07.005

Magnusson R, Arnoldsson K, Lejon C, Hagglund L, Wingfors H (2016) Field evaluation and calibration of a small axial passive air sampler for gaseous and particle bound polycyclic aromatic hydrocarbons (PAHs) and oxygenated PAHs. Environ Pollut 216:235–244. https://doi.org/10.1016/j.envpol.2016.05.067

Maneechakr P, Mongkollertlop S (2020) Investigation on adsorption behaviors of heavy metal ions (Cd^{2+}, Cr^{3+}, Hg^{2+} and Pb^{2+}) through low-cost/active manganese dioxide-modified magnetic biochar derived from palm kernel cake residue. J Environ Chem Eng 8:104467. https://doi.org/10.1016/j.jece.2020.104467

Martins GV, Martins S, Martins AO, Basto MC, Silva GV (2013) Determination of gaseous polycyclic aromatic hydrocarbons by a simple direct method using thermal desorption-gas chromatography-mass spectrometry. Environ Monit Assess 185:6447–6457. https://doi.org/10.1007/s10661-012-3036-8

Matichenkov V, Bocharnikova E (2004) Production practices and quality assessment of food crops: Si in horticultural industry. In: Dris, R., Jain, S.M. (Eds), vol 2. Springer, Dordrecht. https://doi.org/10.1007/1-4020-2536-X_8

Matovic D (2011) Biochar as a viable carbon sequestration option: Global and Canadian perspective. Energy 36:2011–2016. https://doi.org/10.1016/j.energy.2010.09.031

McCammon CS, Woebkenberg ML (2016) General considerations for sampling airborne contaminants. In: NIOSH manual of analytical methods, 5th edn. National Institute for Occupational Safety and Health. https://www.cdc.gov/niosh/nmam/pdf/NMAM_5thEd_EBook-508-final.pdf. Accessed 20 Jan 2025

Meijer SN, Sweetman AJ, Halsall CJ, Jones KC (2008) Temporal trends of polycyclic aromatic hydrocarbons in the U.K. atmosphere: 1991–2005. Environ Technol 42:3213–3218. https://doi.org/10.1021/es702979d

Mitani N, Jian FM, Iwashita T (2005) Identification of the silicon form in xylem sap of rice (Oryza sativa L.). Plant Cell Physiol 46:279–283. https://doi.org/10.1093/pcp/pci018

Mohan D, Sarswat A, Ok YS, Pittman CU (2014) Organic and inorganic contaminants removal from water with biochar, a renewable, low cost and sustainable adsorbent-a critical review. Bioresour Technol 160:191–202. https://doi.org/10.1016/j.biortech.2014.01.120

Mueller A, Ulrich N, Hollmann J, Zapata Sanchez CE, Rolle-Kampczyk UE, von Bergen M (2019) Characterization of a multianalyte GC-MS/MS procedure for detecting and quantifying polycyclic aromatic hydrocarbons (PAHs) and PAH derivatives from air particulate matter for an improved risk assessment. Environ Pollut 255:112967. https://doi.org/10.1016/j.envpol.2019.112967

Mullen CA, Boateng AA, Goldberg NM, Lima IM, Laird DA, Hicks KB (2010) Bio-oil and bio-char production from corn cobs and stover by fast pyrolysis. Biomass Bioenergy 34:67–74. https://doi.org/10.1016/j.biombioe.2009.09.012

Namieśnik J, Zabiegała B, Kot-Wasik A, Partyka M, Wasik A (2005) Passive sampling and/or extraction techniques in environmental analysis: a review. Anal Bioanal Chem Res 381:279–301. https://doi.org/10.1007/s00216-004-2830-8

Nayak S, Raut D, Patnaik L (2019) Naphthalene induced enzymatic alterations in the liver of climbing perch, Anabas testudineus. J Aquat Biol Fish 7:134–141

NIOSH (National Institute for Occupational Safety and Health) (1994) Method 5515: polynuclear aromatic hydrocarbons by GC. https://www.cdc.gov/niosh/docs/2003-154/pdfs/5515.pdf. Accessed 20 Jan 2025

Omidi AH, Cheraghi M, Lorestani B, Sobhanardakani S, Jafari A (2019) Biochar obtained from cinnamon and cannabis as effective adsorbents for removal of lead ions from water. Environ Sci Pollut Res 26:27905–27914. https://doi.org/10.1007/s11356-019-05997-z

Ouchi T, Hamamoto Y, Mori H (2019) Measurement of adsorption/desorption rate of water vapor to a silica gel thin film coated on a surface of a cross-fin tube heat exchanger. Trans JSRAE 36:157–163. https://doi.org/10.11322/tjsrae.19-10DC_OA

Pankow JF (1987) Review and comparative analysis of the theories on partitioning between the gas and aerosol particulate phases in the atmosphere. Atmos Environ 21:2275–2283. https://doi.org/10.1016/0004-6981(87)90363-5

Pankow JF (1988) Gas phase retention volume behavior of organic compounds on the sorbent poly(oxy-m-terphenyl-2',5'-ylene). Anal Chem 60:950–958. https://doi.org/10.1021/ac00160a024

Pankow JF (1994) An absorption model of the gas/aerosol partitioning involved in the formation of secondary organic aerosol. Atmos Environ 28:189–193. https://doi.org/10.1016/1352-2310(94)90094-9

Parnis JM, Mackay D, Harner T (2015) Temperature dependence of Henry's law constants and K_{OA} for simple and heteroatom-substituted PAHs by COSMO-RS. Atoms Environ times 110:27–35. https://doi.org/10.1016/j.atmosenv.2015.03.032

Parr JF (2006) Effect of fire on phytolith coloration. Geoarchaeology 21:171–185. https://doi.org/10.1002/gea.20102

Petrucci RH, William S, Herring FG, Madura JD (2007) General chemistry: principles and modern applications, 9th edn. Pearson Education Inc, Upper Saddle River, New Jersey

Piatt JJ, Backhus DA, Capel PD, Eisenreich SJ (1996) Temperature-dependent sorption of naphthalene, phenanthrene and pyrene to low organic carbon aquifer sediments. Environ Sci Technol 30:751–760. https://doi.org/10.1021/es9406288

Pignatello JJ, Oliveros E, MacKay A (2006) Advanced oxidation processes for organic contaminant destruction based on the fenton reaction and related chemistry. Crit Rev Environ Sci Technol 36:1–84. https://doi.org/10.1080/10643380500326564

Portet-Koltalo F, Oukebdane K, Robin L, Dionnet F, Desbene PL (2007) Quantification of volatile PAHs present at trace levels in air flow by aqueous trapping-SPE and HPLC analysis with fluorimetric detection. Talanta 71:1825–1833. https://doi.org/10.1016/j.talanta.2006.06.043

Qadeer S, Batool A, Rashid A, Khalid A, Samad N, Ghufran M (2014) Effectiveness of biochar in soil conditioning under simulated ecological conditions. Soil Environ 33:149–158 (**Corpus ID: 128455906**)

Qian Y, Posch T, Schmidt TC (2011) Sorption of polycyclic aromatic hydrocarbons (PAHs) on glass surfaces. Chemosphere 82:859–865. https://doi.org/10.1016/j.chemosphere.2010.11.002

Ringuet J, Albinet A, Leoz-Garziandia E, Budzinski H, Vilenave E (2012) Reactivity of polycyclic aromatic compounds (PAHs, NPAHs and OPAHs) adsorbed on natural aerosol particles exposed to atmospheric oxidants. Atmos Environ 61:15–22. https://doi.org/10.1016/j.atmosenv.2012.07.025

Romo D, Velmurugan K, Upham BL, Dwyer-Nield LD, Bauer AK (2019) Dysregulation of gap junction function and cytokine production in response to non-genotoxic polycyclic aromatic hydrocarbons in an in vitro lung cell Model. Cancers 11:572. https://doi.org/10.3390/cancers11040572

Sabino FC, Pinto JP, Amador IR, Martins LD, Solci MC (2016) Gas-phase polycyclic aromatic hydrocarbons in the parking lot impacted by light-duty vehicles burning gasoline and ethanol blends. J Braz Chem Soc 27:1551–1557. https://doi.org/10.5935/0103-5053.20160034

Schwarzenbach RP, Gschwend PM, Imboden DM (2003) Environmental organic chemistry: Chapter 7-Organic liquid-water partition. 2nd Ed., John Wiley & Sons, Inc., Hoboken, New Jersey, pp 213−386

Seinfeld JH, Pandis SN (2006) Atmospheric chemistry and physics: From Air Pollution to climate change, 2nd edn. John Wiley & Sons Inc, Hoboken, New Jersey

Shoeib M, Harner T (2002) Characterization and comparison of three passive air samplers for persistent organic pollutants. Environ Sci Technol 36:4142–4151. https://doi.org/10.1021/es020635t

Sigma-Aldrich Co. (1997) Amberlite XAD-2 Polymeric adsorbent. https://www.sigmaaldrich.com/content/dam/sigmaaldrich/docs/Supelco/Product_Information_Sheet/4802.pdf. Accessed 20 Jan 2025

Sigma-Aldrich Co. (2022) Amberlite® XAD®-2 Polymeric adsorbent. https://www.sigmaaldrich.com/TH/en/product/supelco/10357. Accessed 20 Jan 2025

Singh BP, Zughaibi TA, Alharthy SA, Al-Asmari AI, Rahman S (2023) Statistical analysis, source apportionment, and toxicity of particulate- and gaseous-phase PAHs in the urban atmosphere. Front Public Health 10:1070663. https://doi.org/10.3389/fpubh.2022.1070663

Song W, Guo M (2012) Quality variations of poultry litter biochar generated at different pyrolysis temperatures. J Anal Appl Pyrolysis 94:138–145. https://doi.org/10.1016/j.jaap.2011.11.018

Sonnette A, Millet M, Ocampo R, Alleman L, Coddeville P (2017) Tenax-TA spiking approach of thermal desorption coupled to GC–MSMS for the quantification of PAHs in indoor air and dust. Polycycl Aromat Compd 37:170–177. https://doi.org/10.1080/10406638.2016.1253594

Spicer CW, Holdren MW, Smith DL, Miller SE, Smith RN, Hughes DP (1990) Aircraft emissions characterization: F101 and F110 engines. https://www.researchgate.net/publication/235111468_Aircraft_Emissions_Characterization_F101_and_F110_Engines. Accessed 20 Jan 2025

Spokas KA, Koskinen WC, Baker JM, Reicosky DC (2009) Impacts of woodchip biochar additions on greenhouse gas production and sorption/degradation of two herbicides in a Minnesota soil. Chemosphere 77:574–581. https://doi.org/10.1016/j.chemosphere.2009.06.053

Srogi K (2007) Monitoring of environmental exposure to polycyclic aromatic hydrocarbons: A review. Environ Chem Lett 5:169–195. https://doi.org/10.1007/s10311-007-0095-0

Strandberg B, Österman C, Akdeva HK, Moldanová J, Langerm S (2022) The use of polyurethane foam (PUF) passive air samplers in exposure studies to PAHs in Swedish seafarers. Polycycl Aromat Compd 4:448–459. https://doi.org/10.1080/10406638.2020.1739084

Sukadi AA, Ilyas M (2022) Naphthol as a biological monitoring on naphthalene exposure in workers. IJCOM 1:189–198. https://doi.org/10.53773/ijcom.v1i3.38.189-98

Tala W, Chantara S (2019a) Effective solid phase extraction for highly volatile substances and application for analysis of ambient gaseous PAHs. New J Chem 43:8726–1874. https://doi.org/10.1039/C9NJ04021H

Tala W, Chantara S (2019b) Use of spent coffee ground biochar as ambient PAHs sorbent and novel extraction method for GC-MS analysis. Environ Sci Pollut Res 26:13025–13040. https://doi.org/10.1007/s11356-019-04473-y

Temime B, Francois S, Monod A, Wortham H (2002) An experimental set up of a PAH vapor generator and its use to test an annular

denuder. Environ Pollut 120:609–616. https://doi.org/10.1016/S0269-7491(02)00193-8

Temime-Roussel B, Monod A, Massiani C, Wortham H (2004) Evaluation of an annular denuder for atmospheric PAH partitioning studies-2: evaluation of mass and number particle losses. Atmos Environ 38:1925–1932. https://doi.org/10.1016/j.atmosenv.2004.01.006

US EPA (United State Environmental Protection Agency) (1999) Compendium method TO-13A: determination of polycyclic aromatic hydrocarbons (PAHs) in ambient air using gas chromatography/mass spectrometry (GC/MS). https://www.epa.gov/sites/production/files/2019-11/documents/to-13arr.pdf. Accessed 20 Jan 2025

Wang J, Wang S (2019) Preparation, modification and environmental application of biochar: a review. J Clean Prod 227:1002–1022. https://doi.org/10.1016/j.jclepro.2019.04.282

Wang L, Yang Z, Niu J (2011) Temperature-dependent sorption of polycyclic aromatic hydrocarbons on natural and treated sediments. Chemosphere 82:895–900. https://doi.org/10.1016/j.chemosphere.2010.10.054

Wang X, Zhou W, Liang G, Song D, Zhang Z (2015) Characteristics of maize biochar with different pyrolysis temperatures and its effects on organic carbon, nitrogen and enzymatic activities after addition to fluvo-aquic soil. Sci Total Environ 538:137–144. https://doi.org/10.1016/j.scitotenv.2015.08.026

Waterken L, Bienfait A, Peeters A (1981) Epidermal callose and silica: relationships with cuticular transpiration. Cell 73:265–287. (In French)

Wauters E, Van Caeter P, Desmet G, David F, Devos C, Sandra P (2008) Improved accuracy in the determination of polycyclic aromatic hydrocarbons in air using 24 h sampling on a mixed bed followed by thermal desorption capillary gas chromatography–mass spectrometry. J Chromatogr A 1190:286–293. https://doi.org/10.1016/j.chroma.2008.02.081

Wei MC, Chang WT, Jen JF (2007) Monitoring of PAHs in air by collection on XAD-2 adsorbent then microwave-assisted thermal desorption coupled with headspace solid-phase microextraction and gas chromatography with mass spectrometric detection. Anal Bioanal Chem Res 387:999–1005. https://doi.org/10.1007/s00216-006-0962-8

Wei W, Mandin C, Blanchard O, Mercier F, Pelletier M, Le Bot B, Glorennec P, Ramalho O (2016) Temperature dependence of the particle/gas partition coefficient: An application to predict indoor gas-phase concentrations of semi-volatile organic compounds. Sci Total Environ 563–564:506–512. https://doi.org/10.1016/j.scitotenv.2016.04.106

Weschler CJ, Salthammer T, Fromme H (2008) Partitioning of phthalates among the gas phase, airborne particles and settled dust in indoor environments. Atmos Environ 42: 1449e1460. https://doi.org/10.1016/j.atmosenv.2007.11.014

Wong P, Laxton V, Srivastava S, Chan YWF, Tse G (2017) The role of gap junctions in inflammatory and neoplastic disorders (Review). Int J Mol Med 39:498–506. https://doi.org/10.3892/ijmm.2017.2859

Xie M, Hannigan MP, Barsanti KC (2014) Gas/particle partitioning of n-alkanes, PAHs and oxygenated PAHs in urban Denver. Atmos Environ 95:355–362. https://doi.org/10.1016/j.atmosenv.2014.06.056

Xu Y, Zhang YL, Li J, Gioia R, Zhang G, Li XD, Spiro B, Bhatia RS, Jones KC (2012) The spatial distribution and potential sources of polycyclic aromatic hydrocarbons (PAHs) over the Asian marginal seas and the Indian and Atlantic Oceans. J Geophys Res Atmos 117:D07302. https://doi.org/10.1029/2011JD016585

Xu H, Zhan M-X, Cai P-T, Ji L-J, Chen T, Li X-D (2019) Adsorption characteristics of polycyclic aromatic hydrocarbons by biomass-activated carbon in flue gas. Energy Fuels 33:11477–11485. https://doi.org/10.1021/acs.energyfuels.9b02723c

Yang H, Shi Z, Wang XX, Cheng R, Lu M, Zhu J, Zhang SY (2019) Phenanthrene, but not its isomer anthracene, effectively activates both human and mouse nuclear receptor constitutive androstane receptor (CAR) and induces hepatotoxicity in mice. Toxicol Appl Pharm 378:114618. https://doi.org/10.1016/j.taap.2019.114618

Zama EF, Zhu Y-G, Reid BJ, Sun G-X (2017) The role of biochar properties in influencing the sorption and desorption of Pb (II), Cd (II) and As (III) in aqueous solution. J Clean Prod 148:27–136. https://doi.org/10.1016/j.jclepro.2017.01.125

Zand AD (2017) Leaching characteristics of phenanthrene and pyrene in biochar-amended contaminated soil. J Appl Biotechnol Rep 4:573–581 (**Corpus ID: 89875732**)

Zaranski MT, Patton GW, McConnell LL, Bidleman TF (1991) Collection of nonpolar organic compounds from ambient air using polyurethane foam-granular adsorbent sandwich cartridges. Anal Chem 63:1228–1232. https://doi.org/10.1021/ac00013a009

Zhang X, Wang H, He L, Lu K, Sarmah A, Li J, Bolan NS, Pei J, Huang H (2013) Using biochar for remediation of soils contaminated with heavy metals and organic pollutants. Environ Sci Pollut Res 20:8472–8483. https://doi.org/10.1007/s11356-013-1659-0

Zheng J, Yang C, Xue M, Li X, Zhao X (2024) Mass transfer kinetics of volatile organic compound desorption from a novel adsorbent. Processes 12:2031. https://doi.org/10.3390/pr12092031